

1 Differences in MOPITT surface-level CO retrievals and trends from Level 2 and Level 2 3 products in coastal grid boxes

3

4 Ian Ashpole¹ and Aldona Wiacek^{1,2}

5

6 ¹Department of Environmental Science, Saint Mary's University, Halifax, Canada

7 ²Department of Astronomy and Physics, Saint Mary's University, Halifax, Canada

8 *Correspondence to:* Ian Ashpole (ian.ashpole@smu.ca)

9

10

11 Abstract

12

13 MOPITT retrievals are more sensitive to near-surface CO when performed over land than water. Data users
14 are therefore advised to discard retrievals performed over water from analyses to limit the a priori influence
15 on results. Level 3 (L3) products are a 1° x 1° gridded average of finer resolution Level 2 (L2) retrievals. For
16 coastal grid boxes, these are retrievals that are either performed over land, water, or a combination of the
17 two, on any given day. L3 data users therefore have limited ability to filter for retrievals performed over
18 water for these grid boxes. The consequences that this has on surface-level retrievals and their temporal trends
19 in “as-downloaded” L3 data (“L3O”) are examined in this paper, for all coastal L3 MOPITT grid boxes (n =
20 4299), by comparison to separate land- and water-only grid box averaged L2 retrievals (“L3L” and “L3W”,
21 respectively). First, it is established that mean retrieved VMRs in L3L and L3W differ by over 10 ppbv,
22 significant (p < 0.1) at 60 % of the coastal grid boxes. Trends are also stronger in L3L (mean difference
23 between 0.28 ppbv y⁻¹ and 0.43 ppbv y⁻¹), with the L3L – L3W trend difference significant at 36 % of grid
24 boxes. These L3L – L3W differences are clearly linked to retrieval sensitivity differences, with L3W being
25 more heavily tied to the a priori CO profiles used in the retrieval, which are a model-derived monthly mean
26 climatology that, by definition, has no trend year-to-year. On days when L3O is created from the averaging
27 together of L2 retrievals over both land and water (L3O_M), the result is VMRs that are significantly different
28 to L3L for 45 % of all coastal grid boxes, corresponding to 75 % of grid boxes where the L3L – L3W
29 difference is also significant. Just under half of the grid boxes that featured a significant L3L – L3W trend
30 difference also see trends differing significantly between L3L and L3O_M. Factors that determine whether
31 L3O_M and L3L differ significantly include proportion of the surface covered by land/water, and the
32 magnitude of sensitivity contrast. Comparing the full L3O dataset to L3L, it is shown that if L3O is filtered
33 so that only retrievals over land (L3O_L) are analysed, there is a huge loss of days with data. This is because
34 L2 retrievals over land are routinely discarded during the L3O creation process, for coastal grid boxes. The

35 problem can be lessened by also retaining L3O_M retrievals, but the resulting L3O “land or mixed” (L3O_{LM})
36 subset still has less data days than L3L for 61 % of coastal grid boxes. Moreover, these additional days with
37 data feature some influence from retrievals made over water that can affect results. Coastal L3 grid boxes
38 contain 33 of the 100 largest coastal cities in the world, by population. Focusing on the L3 grid boxes
39 containing these cities, we ask whether results of analyses are significantly different if using L3O compared
40 to L3L. It is shown that mean VMRs in L3O_L and L3L differ significantly for 11 of the 27 grid boxes that
41 can be compared (there are no L3O_L data for 6 of the grid boxes studied). The L3L – L3O_{LM} mean VMR
42 difference exceeds 10 (22) ppbv for 11 (3) of the 33 grid boxes, significant in 13 cases. 9 of the 18 grid boxes
43 where WLS analysis can be performed in L3O_L feature a trend that is significantly different to L3L. The
44 trends in L3O_{LM} and L3L differ significantly for 5 of the 33 grid boxes. It is concluded that a L3 product
45 based only on L2 retrievals over land – [the L3L product analysed in this paper, available for public download](#)
46 – [would](#) be of benefit to MOPITT data users, given the significant differences in mean CO VMRs and trends
47 that can be obtained for coastal grid boxes using L2 products in which retrievals performed over water can
48 be more easily discarded.

49
50

51 **1. Introduction**

52

53 Carbon monoxide (CO) is directly emitted into the atmosphere from anthropogenic (e.g. fossil fuel burning)
54 and natural (e.g. wildfire) sources, and also produced via the oxidation of hydrocarbons in the atmosphere.
55 With an atmospheric lifetime of weeks to months (e.g. Duncan et al., 2007), it is an important tracer of
56 pollutant transport and indicator of emission sources. While a health concern in its own right at high enough
57 concentrations, CO also plays an important role in atmospheric chemistry, for example as a precursor to
58 ozone formation and a primary sink for the hydroxyl radical. Atmospheric CO concentrations have decreased
59 since the start of the 21st century, with a slowdown in the rate of decline observed in recent years (Buchholz
60 et al., 2021). Trends also show substantial spatial variability (Hedelius et al., 2021). Satellite instruments
61 have been central to our understanding of global change in CO concentrations, with the Measurement of
62 Pollution in the Troposphere (MOPITT – Drummond et al., 2010, 2016) instrument well suited to this task,
63 providing a nearly-unbroken and consistent data record since the year 2000.

64 MOPITT observes upwelling radiances at thermal infrared (TIR) and near infrared (NIR) wavelengths
65 and uses these in an optimal estimation retrieval algorithm to retrieve coarse vertical resolution CO profiles,
66 which are integrated to give total column amounts. Among multiple additional inputs required by the retrieval
67 algorithm, a priori CO profiles – which describe the most probable state of the CO profile at a given location
68 – are necessary to constrain the retrieval to physically reasonable limits (Pan et al., 1998; Rodgers, 2000; the

69 retrieval algorithm is outlined in more detail in Sect. 2.1). For the most recent iterations of MOPITT products,
70 these a priori CO profiles are based on a monthly climatology from a chemical transport model. The degree
71 to which a given MOPITT retrieval reflects information obtained from the observed radiances – known as
72 “information content” – is highly spatially and temporally variable, depending on scene-specific factors such
73 as surface temperature, thermal contrast in the lower troposphere, and the actual (“true”) CO loading itself,
74 as well as on instrumental noise (e.g. Deeter et al., 2015). The lower the retrieval information content, the
75 closer the retrieved CO loading will be to the a priori; a model value.

76 Retrievals that take place over water are known to have a lower information content than retrievals
77 that take place over land. Primarily, this is due to weak thermal contrast near to the surface hampering the
78 instrument’s ability to sense CO absorption in the lowermost layers of the troposphere (Deeter et al., 2007;
79 Worden et al., 2010), and this is confounded by a lack of NIR reflectance over water, which limits these
80 retrievals to TIR wavelengths only. It is therefore recommended that MOPITT data users exclude these
81 retrievals from any analyses they perform, to ensure that results are not biased by retrievals that have a heavy
82 reliance on the a priori (MOPITT Algorithm Development Team, 2018; Deeter et al., 2015). Such filtering
83 is specifically emphasised where the focus of analysis is the identification of long-term CO trends, because
84 any real trends in the data will be weakened by the inclusion of retrievals that are tied heavily to the a priori
85 (Deeter et al., 2015). This is because the a priori CO profiles are taken from monthly modelled CO
86 climatologies: for a given location and day of the year, they will be the same every year and therefore feature
87 no temporal trend (Deeter et al., 2014).

88 MOPITT data are available as either Level 2 (“L2”) or Level 3 (“L3”) products. L2 products contain
89 each individual retrieval, at ~22 x 22 km spatial resolution. L3 products are a 1° x 1° gridded area-average of
90 the individual L2 retrievals that fall within each grid box (see Fig. 1), with some filtering criteria applied.
91 One criterion is the surface type over which the L2 retrievals were performed – either land, water, or “mixed”.
92 If more than 75 % of the bounded L2 retrievals were performed over the same surface type then only those
93 retrievals are averaged to create the L3 product and the rest are discarded; otherwise, all bounded L2 retrievals
94 are averaged, and the L3 product is given the surface type classification of “mixed” (L3 surface type
95 classification is explained in more detail in Sect. 2.2). This creates a problem for L3 grid boxes that overlay
96 coastlines: To a greater or lesser extent, these L3 products will have some contribution from L2 retrievals
97 performed over water, as shown in Fig. 1. L3 product users have limited capability to discard them, at least
98 without sacrificing temporal resolution, because each L3 grid box only has a single “retrieval” per day. By
99 contrast, with L2 products it is possible, for the same coastal grid boxes, to choose to retain only the retrievals
100 performed over land. In practical terms, this means that, for coastal L3 grid boxes, valuable retrieval
101 information over land, available in L2 products, can be lost to users of L3 products.

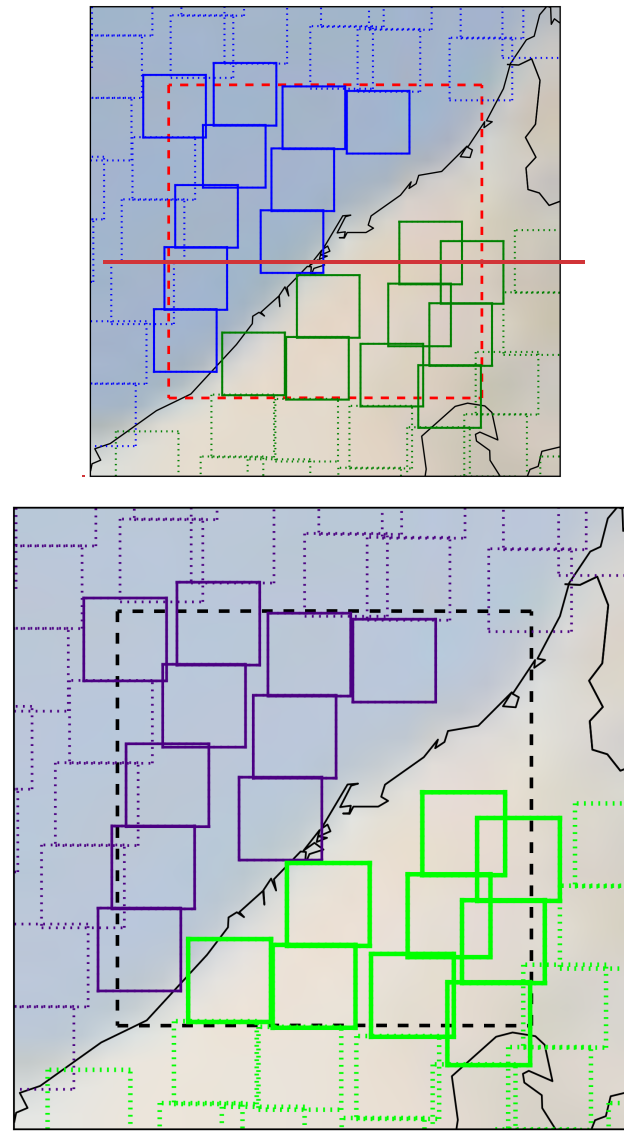


Figure 1. Example of a coastal L3 grid box (red-black dashed box) and bounded L2 retrievals from which the L3 products for that grid box are created. Blue-Purple (green) boxes correspond to L2 retrievals with a surface index of “water” (“land”). Note that only L2 retrievals with a midpoint that falls within the boundaries of the L3 grid box will be used in L3 creation for that grid box. These are indicated by solid blue/purple/green outlines – those not included in L3 creation for this grid box are shown with dotted blue/purple/green outlines. More information on surface indexing and L3 product creation is given in Sect. 2.2. “Coastal” L3 grid box classification is outlined in Sect. 2.3. The coastal L3 grid box visualized here contains the city of Dubai (~centre = 55.296° E, 25.277° N), which features in the case study analysis of Sect 3.4. Faint background shading is from Nasa Blue Marble imagery.

102 With a focus on the coastal L3 grid box containing the city of Halifax, Canada, Ashpole and Wiacek
 103 (2020) demonstrate the consequences of this loss of retrieval information in L3 products. They compare the

104 results of analyses performed using L3 data and L2 data whereby only bounded retrievals performed over
105 land were retained, and find significant differences in both seasonal mean statistics and the magnitudes of
106 trends identified in surface-level CO. These differences are a direct result of the L3 products being dominated
107 by L2 retrievals over water, which feature a weaker trend than the L2 retrievals over land, demonstrably due
108 to a greater a priori influence owing to their reduced true-profile sensitivity. In their conclusions, Ashpole
109 and Wiacek (2020) suggest that L2 retrievals over water should not contribute to L3 products for coastal grid
110 boxes, which would be consistent with previous data filtering recommendations (MOPITT Algorithm
111 Development Team, 2018; Deeter et al., 2015). The primary aim of this paper is to explore the extent of the
112 difference that this would make on a global scale. This is necessary to understand for two reasons: firstly, L3
113 data are more convenient for long time series analysis than L2 data owing to their smaller file size (~25 MB
114 vs ~450 MB respectively, for a single daily, global file). It cannot be overlooked that working with L3 data
115 thus requires fewer computing resources and less technical proficiency, with a range of simple-to-use tools
116 available for working with gridded products. L3 products thus make the MOPITT data more easily accessible,
117 especially to less-expert users, who may lack the expertise required to scrutinize the data for potential a priori
118 bias. Secondly, many of the world’s largest agglomerations are situated within a coastal L3 grid box (5 of
119 the top 10 and 33 of the top 100 largest agglomerations by population; derivation outlined in Sect. 2.5),
120 making these likely targets for analyses of air quality indicators, especially their changes over time.

121 This paper presents a comparison of results from analyses performed using [original, “as downloaded”](#)
122 [L3 data products](#), and [a new separate land-only ~~and water-only~~ L3 product \(“L3L”, Ashpole and Wiacek](#)
123 [\(2022\) – outlined in Sect. 2.4\) that has been created ~~area averages~~](#) from L2 products, for all MOPITT L3 grid
124 boxes that overlay coastlines [\(a water-only L3 product “L3W” has also been created for comparison](#)
125 [purposes\) \(“L3L” and “L3W” respectively – derivation outlined in Sect. 2.4\). Section 2 describes the datasets](#)
126 [and methods used, including outlining the creation of the new L3L and L3W data products analysed in this](#)
127 [paper](#). Section 3.1 demonstrates the magnitude of the sensitivity difference for retrievals over land and water,
128 zooming in to focus on coastal grid boxes (the classification of which is outlined in Sect. 2.3). Section 3.2
129 links the sensitivity contrast to differences in mean CO volume mixing ratios (“VMRs”) and their temporal
130 trends for L2 retrievals performed over land and water within coastal L3 grid boxes; and evaluates the effect
131 that the averaging together of these retrievals has on the statistics and trends in resulting L3 “mixed” values.
132 Section 3.3 quantifies the proportion of L2 retrievals performed over land within coastal L3 grid boxes that
133 are lost to L3 products, before finally comparing statistics and trends in L3 and L2 products for all coastal
134 L3 grid boxes, outlining the magnitude and significance of differences for the coastal grid boxes that contain
135 33 of the largest 100 cities in the world (Sect. 3.4).

136

137

138 **2. Data and Methods**

139

140 **2.1. MOPITT Instrument and retrieval overview**

141

142 Carried on board the polar-orbiting NASA Terra satellite that was launched in December 1999, MOPITT
143 began measuring CO in March 2000 and has provided near-continuous measurements to date. With a native
144 pixel resolution of $\sim 22 \times 22$ km at nadir and a swath width of ~ 640 km, it offers near global coverage roughly
145 every 3-days, crossing the equator at $\sim 10:30$ and $\sim 22:30$ local time. The instrument is a gas correlation
146 radiometer that measures radiances in two CO-sensitive spectral bands: the TIR at $4.7 \mu\text{m}$, which is sensitive
147 to both absorption and emission by CO and can provide information on its vertical distribution in the
148 troposphere; and the NIR at $2.3 \mu\text{m}$, which constrains the CO total column amount and yields information
149 on CO concentrations in the lower troposphere (LT), to which TIR radiances are typically less sensitive
150 (Drummond et al., 2010; Pan et al., 1995, 1998). For the work presented here, the TIR-NIR combined
151 MOPITT product is used, owing to its demonstrably greater sensitivity to CO loadings near to the surface
152 than the TIR- and NIR- only products which are also available (Deeter et al., 2013). Note, however, that
153 retrievals over water and at night are limited to the TIR band only due to the lacking NIR signal. This analysis
154 is based on daytime-only retrievals (more information on data selection and preparation is given in Sect. 2.4).

155 Multiple other sources describe the retrieval algorithm in detail (e.g., Deeter et al., 2003; Francis et
156 al., 2017). In short, it uses optimal estimation (Pan et al., 1998; Rogers, 2000) and a fast radiative transfer
157 model (Edwards et al., 1999) to invert measured radiances and retrieve the CO volume mixing ratio (VMR)
158 profile on 10 vertical layers. The vertical grid consists of 9 equally spaced pressure levels from 900 to 100
159 hPa (the uppermost level covers the atmospheric layer from 100 to 50 hPa), with a floating surface pressure
160 level (if the surface pressure is below 900 hPa, less than 10 profile levels are retrieved). Retrieved values
161 represent the mean CO VMR in the layer immediately above that level. These profile measurements are then
162 integrated to provide total column CO amounts. Retrievals are only performed for scenes free of cloud (cloud
163 clearing is based on coincident MODIS observations and MOPITT's own radiances).

164 In addition to the measured radiances, the retrieval requires multiple inputs including meteorological
165 data, surface temperature and emissivity, and, of direct relevance to this study, a priori CO profiles, which
166 are necessary to constrain the retrieval to physically reasonable limits. These a priori CO profiles come from
167 a monthly CO climatology (years 2000-2009), simulated with the Community Atmosphere Model with
168 Chemistry (CAM-chem) chemical transport model (Lamarque et al., 2012) at a spatial resolution of $1.9^\circ \times$
169 2.5° , which is then spatially and temporally interpolated to the time and location of each individual MOPITT

170 observation. A priori profiles for a given location and day of the year are therefore the same every year and
171 feature no temporal trend. To understand the physical significance of the MOPITT CO retrievals, it is
172 necessary to examine the retrieval Averaging Kernels (AKs), available with all MOPITT data products,
173 which quantify the sensitivity of the retrieved vertical profile to the “true” vertical profile. The lower the
174 retrieval sensitivity, the greater the a priori weighting. Two different components of AKs are analysed in this
175 paper: AK rowsums, which represent the overall sensitivity of the retrieved profile at the corresponding
176 pressure level to the whole true profile; and AK diagonal values, which represent the sensitivity of the
177 retrieved profile at the corresponding pressure level to the same level of the true profile (e.g. the AK diagonal
178 value for the surface level of the retrieved profile represents its sensitivity to the surface level of the true
179 profile).

180 From time-to-time, new MOPITT products become available as improvements are made to the
181 retrieval algorithm and radiative transfer model, yielding superior validation statistics compared to earlier
182 product versions (Worden et al., 2014). This analysis uses MOPITT Version 8 (V8) products (Deeter et al.,
183 2019). Note that Version 9 (V9) products became available shortly after this study was completed. V9
184 features cloud screening improvements that yield additional retrievals over land in comparison to V8 (the
185 exact percent change varies significantly with geography). Validation results are comparable to V8. An
186 overview of MOPITT V9 is given by Deeter et al (2022⁺). A subset of the analysis presented in this paper
187 has been duplicated using V9 data, and this confirms that the main conclusions drawn based on V8 data also
188 hold for V9 (this analysis is outlined in the Supp. Mat. (SM1)). This is to be expected, given that the land-
189 water sensitivity contrast remains in V9 and the L3 processing method is unchanged.

190

191

192 **2.2. MOPITT surface type classification**

193

194 To aid in filtering and interpreting retrievals, all MOPITT data products are distributed with a range of
195 diagnostic fields. As retrieval information content is known to be variable depending on the type of surface
196 over which it is performed (Deeter et al., 2007), L2 retrievals are given a surface index according to whether
197 they were performed over land, water, or a combination of the two (“mixed”). For a given 1° x 1° L3 grid
198 box, how the L2 retrievals that fall within its boundaries are processed to produce the L3 product depends on
199 how their surface indexes vary: If more than 75 % of the bounded L2 retrievals have the same surface index,
200 only those retrievals are averaged to produce the L3 gridded value, and the L3 surface index is set to that
201 surface type (the other L2 retrievals are discarded). Otherwise, all L2 retrievals available in the L3 grid box
202 are averaged together and the L3 surface index is set to “mixed”, as is the case in the example shown in Fig.

203 1 (this information is taken from the MOPITT Version 6 L3 data quality summary¹, which at the time of
204 writing, is the most recent data quality summary to detail exactly how L3 data are created, despite more
205 recent data quality summaries being available). Note that the L2 VMR profiles that are averaged to produce
206 the L3 retrieval are first converted to log(VMR) profiles, then averaged, and the mean log(VMR) profile is
207 then converted back to a VMR profile.

208 Each L3 grid box only has one retrieval per day. This dictates that where the grid box overlies both
209 land and water, its surface index could vary through time, depending on the population of L2 retrievals from
210 which it is created. The make-up of this population can also vary from day-to-day due to factors such as cloud
211 cover, and screening for data quality issues: on day n the population could be predominantly L2 retrievals
212 over land, on day $n+1$ it could be predominantly L2 retrievals over water, and on day $n+2$ it could be an even
213 mix of the two. Given that the averaging together of retrievals with significantly different sensitivity profiles
214 – as could be the case when averaging retrievals over land and water – serves to dilute the information coming
215 from the MOPITT observed radiances with information coming from the a priori and is therefore discouraged
216 (MOPITT Algorithm Development Team, 2018; Deeter et al., 2015; Deeter et al., 2007); and that MOPITT
217 data users are advised to exclude retrievals over water from analyses owing to the known reduced sensitivity,
218 this introduces two potential problems for L3 data taken from coastal grid boxes: firstly, discarding all L3
219 retrievals with the surface index of water will result in a loss of temporal coverage; secondly, L3 retrievals
220 with a surface index of mixed feature some contribution from L2 retrievals over water. The consequences of
221 both these problems are explored in this paper.

222
223

224 **2.3. Coastal grid box classification for this study**

225

226 Since the focus of this paper is on “coastal” L3 grid boxes, it is first necessary to isolate these from the
227 remaining “land-only” or “water-only” L3 grid boxes in the MOPITT data set. The initial step is to identify
228 all grid boxes that have a surface index of “mixed” at least once during the study period. This indicates that
229 the ground area within those grid boxes was both land and water. However, analysis of the global distribution
230 of L3 grid boxes featuring a surface index of mixed revealed that, in addition to actual coastlines, a large
231 proportion of inland grid boxes that are clearly not coastal (“false coastal”) are given the surface index of
232 mixed at least some of the time (Fig. 2a). The reason for this is unclear, but it could be for real physical
233 reasons, such as land grid boxes sporadically flooding, or due to issues in the retrieval schemes caused by
234 e.g. cloud screening problems or the presence of surface ice cover. One characteristic of these false coastal

¹ available here: https://eosweb.larc.nasa.gov/sites/default/files/project/mopitt/quality_summaries/mopitt_level3_ver6.pdf

235 grid boxes is that, compared to the total number of days with L3, the relative frequency with which they are
236 flagged as land is very high (expressed as the ratio “n_days(L3O_L/L3O)”, plotted in Fig. 2b). This relative
237 frequency is much lower for “true” coastal grid boxes, to be expected given prior knowledge of 1) the fact
238 that these grid boxes span both land and water surface types; and 2) how the surface index is determined for
239 L3 data (as outlined in Sect. 2.2). Following iterative threshold testing, L3 coastal grid boxes are classified
240 as grid boxes that:

241

- 242 1. Have at least one classification of “mixed” during the study period
- 243 2. Have an n_days(L3O_L/L3O) ratio < 0.5.

244

245 The distribution of coastal grid boxes identified using these criteria is shown in Fig. 2c. Most false coastal
246 grid boxes are removed, although there are still some erroneous classifications evident, mostly in the north
247 of Canada and Russia. However, placing a more restrictive threshold on the n_days(L3O_L/L3O) ratio to

248 remove these areas has diminishing returns since it results in the rejection of more true coastal grid boxes.
249 These criteria therefore strike a balance between minimising false and maximising true classifications.

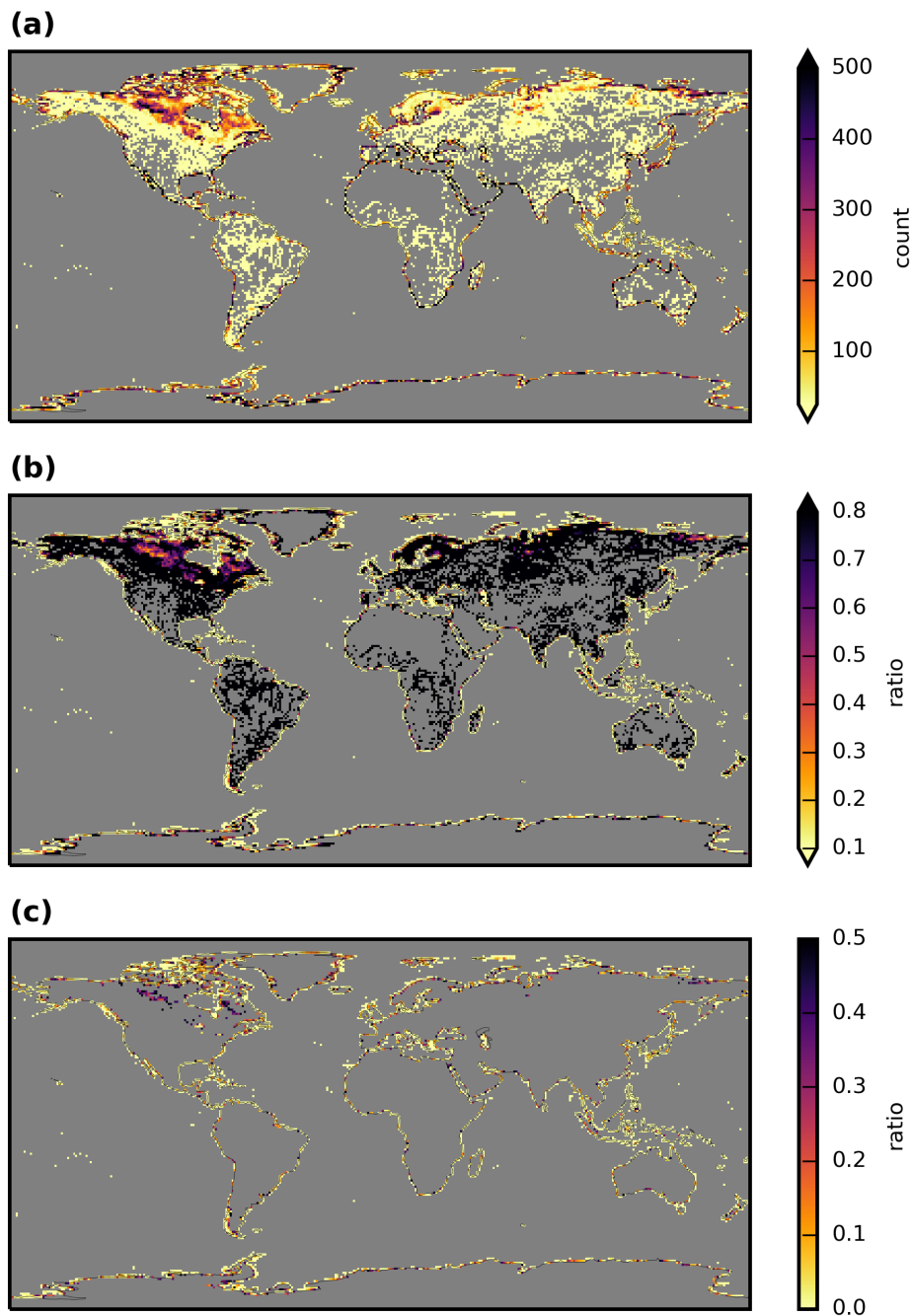


Figure 2. Maps showing the stages of derivation of the coastal L3 grid box mask applied in this paper to MOPITT data. **(a)** Frequency with which L3 grid boxes are given the surface index of “mixed”, calculated from daily data between 2001-08-25 and 2019-02-28. **(b)** Frequency with which L3 grid boxes that have a surface index of “mixed” at least once in panel a have the surface index of “land”, compared to the total number of days with which L3 data are available for that grid box (expressed as $n_days(L3O_L/L3O)$). **(c)** As b, but with a threshold of $n_days(L3O_L/L3O) < 0.5$ applied. This is the coastal L3 grid box mask used in this paper.

250 Applying these criteria to the MOPITT L3 data yields 4299 coastal grid boxes, from a total of 64800
251 L3 grid boxes (6.6 %). This mask is applied to all data, and only those L3 grid boxes that remain are classified
252 as coastal. Only data for these coastal grid boxes are analysed in this study (with the exception of global L3
253 maps analysed in Sect. 3.1.1).

254
255

256 **2.4. MOPITT datasets analysed, and data processing method for creating land- and water-only L3** 257 **products (“L3L” and “L3W”)** 258

259 All available MOPITT V8 Level 2 (L2) and Level 3 (L3) daily TIR-NIR files (“MOP02J” and “MOP03J”
260 files, respectively) were downloaded from the NASA Earthdata portal (<https://search.earthdata.nasa.gov>).
261 Although the data record begins in March 2000, analysis is restricted to the period from 2001-08-25 to 2019-
262 02-28. Data prior to 2001-08-25 are discarded due to an instrumental reconfiguration in 2001 creating an
263 inconsistency in the data record (Drummond et al., 2010). Data post 2019-02-28 are flagged as “beta” at the
264 time of writing, their use in scientific analysis (especially for examining long-term records of CO) being
265 discouraged until final processing and calibration occurs (MOPITT Algorithm Development Team, 2018).
266 For clarity, the original, “as-downloaded” L3 time series is referred to as “L3O” for the remainder of this
267 paper. Only retrievals that were performed during daytime hours are retained (daytime and nighttime
268 retrievals are stored as separate fields in MOP03J files). For this analysis, separate subsets of L3O are created
269 according to surface index: L3O land-only (“L3O_L”), L3O water-only (“L3O_W”), L3O mixed (“L3O_M”), L3O
270 land-or-mixed (“L3O_{LM}”). When the L3O dataset is analysed with no filtering by surface index applied, it is
271 referred to as “L3O_{NF}”.

272 The land- and water-only L3 products are created from daily L2 data. The first step of L2 data
273 processing ~~for this study~~ required is to filter the retrievals as is done for the processing of ~~at the~~ L3O
274 ~~processing stage~~. This involves:

275

- 276 • Discarding all observations for Pixel 3 (this corresponds to one of MOPITT’s four detectors);
- 277 • Discarding all observations where both (1) the channel 5A signal-to-noise-ratio (“SNR”) < 1000 and
278 (2) the channel 6A SNR < 400 (5A and 6A correspond to the average radiances for MOPITT’s length-
279 modulated cell TIR and NIR channels, respectively)

280

281 This filtering takes place because observations from specific elements on MOPITT’s detector array were
282 found to exhibit greater retrieval noise than the other elements, and their inclusion therefore lowered overall

283 L3 information content (MOPITT Algorithm Development Team, 2018). Only daytime L2 retrievals are
284 retained, using a solar zenith angle filter of $< 80^\circ$.

285 From the remaining set of filtered L2 retrievals, separate area averages are taken for those with a
286 surface index of land and water, for every $1^\circ \times 1^\circ$ L3 grid box. This effectively creates two new L3 “land-
287 only” and “water-only” products, which are referred to herein as “L3L” and “L3W”. For clarity of analysis,
288 remaining L2 retrievals with a surface index of mixed are discarded. These make up a very small proportion
289 of the overall L2 retrievals (e.g. $< 5\%$ for the grid box containing Halifax, analysed in Ashpole and Wiacek,
290 2020). [Both L3L and L3W are publicly available for download \(Ashpole and Wiacek, 2022\)](#). Note that, as
291 with the creation of L3O, L2 VMR profiles for each L3 grid box are first converted to $\log(\text{VMR})$ profiles
292 before averaging, and the mean $\log(\text{VMR})$ profile is then converted back to a VMR profile to give the final
293 L3L and L3W retrievals. [Additionally, the number of L2 retrievals that are used for calculating the area
294 averages when creating L3L and L3W \(“n_ret_L” and “n_ret_W”, respectively\) is recorded. The ratio
295 n_ret_L/n_ret_W \(herein referred to as “ratio\(land/water\)” for simplicity\) is used to indicate the proportion of
296 the L3 grid box that is covered by land vs water: a ratio of 1 indicates an even split of these surface types in
297 the grid box; a ratio \$< 1\$ indicates that a greater proportion of its surface is water covered; and a ratio \$> 1\$
298 indicates that the grid box is land-dominated.](#)

299 From these L3O, L3L, and L3W datasets, only grid boxes that are classified as “coastal” using the
300 coastal grid box masked outlined in Sect. 2.3 are analysed.

301 Note that the analysis presented in this paper is restricted to daily products. Monthly L3 files are
302 available, however the absence of a monthly L2 product precludes the analysis from being conducted on
303 those data. Based on the results of the analysis of daily data, however, there is reason to also advise caution
304 if working with coastal grid boxes in the monthly L3 product. This is because the data for those grid boxes
305 will still be created from daily L2 retrievals over land and water, with the same implications that are discussed
306 in this paper.

307

308

309 **2.5. Time series preparation, statistical methods, and additional data sources**

310

311 For every coastal L3 grid box, two separate time series from each of the L3O, L3L, and L3W datasets are
312 analysed:

313

- 314 1. The time series analysed in Sect. 3.1 and 3.2 only contain days where L3L and L3W are both present
315 and the L3O surface index is mixed (“L3O_M”). This is to ensure that the true CO profiles are as similar

316 as possible when directly comparing L3L and L3W for a given coastal grid box. Furthermore, it
317 allows for the analysis of the resulting L3O_M data on these days with knowledge of the parent L2
318 retrievals over land and water and their differences.

- 319
- 320 2. In Sect. 3.3 and 3.4 the full time series from each dataset is analysed with no temporal filtering
321 applied.

322

323 Descriptive statistics are calculated from both time series across the whole study time period, and also
324 for individual years (full years only – 2002 to 2018 inclusive) in order to perform the regression analysis
325 outlined below.

326 To identify and compare temporal trends for each coastal grid box in the datasets outlined above,
327 weighted least squares (WLS) regression analyses is performed on yearly mean values, weighted by the
328 inverse of the standard deviation of the measurements used in the yearly mean (i.e. $1/\sigma$). For years that contain
329 just a single retrieval, the weighting is set to $1/100000$ to de-weight them in the fit. If there are more than 2
330 years in a time series for a given grid box that have no data, the regression analysis is not performed. WLS
331 is preferred over OLS because it is less sensitive to outliers. For simplicity, no other trend detection methods
332 – e.g. the Thiel-Sen slope estimator – are applied to corroborate the trends that are detected with WLS, nor
333 do we analyse additional datasets to verify them. Such extra steps would be necessary if the actual trend
334 values were the focus of this study; however, the aim of this trend analysis is instead to identify whether the
335 same method can yield different results depending on which of L3O, L3L or L3W is analysed. [Trend
336 verification is beyond the scope of this study.](#)

337 To determine whether two trends identified are significantly different, their difference is evaluated
338 using the Z test as follows:

339

$$340 Z = \frac{Trend_1 - Trend_2}{\sqrt{SE_1^2 + SE_2^2}}$$

341

342 where SE_1 and SE_2 correspond to the standard errors of $Trend_1$ and $Trend_2$ respectively, and Z is the test
343 statistic. Where Z is greater (less) than 1.645 (-1.645) the trend difference is statistically significant to at least
344 90 % (i.e. $p < 0.1$). In addition, two trends are classified as being significantly different if $Trend_1$ is
345 significantly different to zero ($p < 0.1$) but $Trend_2$ is not ($p > 0.1$), and vice-versa (i.e. the conclusion would
346 be that $Trend_1$ is not zero, but $Trend_2$ may be).

347 A list of the top 100 largest agglomerations by population in the world is obtained from
348 <http://www.citypopulation.de/> (valid at time of writing). 33 of these are situated in a coastal grid box,
349 according to the classification in Sect. 2.3. Time series of L3L, L3W, and L3O are extracted from each of
350 these grid boxes for the analysis in Sect. 3.4.

351

352

353

354

355

356 **3. Results and Discussion**

357

358 **3.1. Land-water contrast in MOPITT sensitivity**

359

360 This section demonstrates the land-water sensitivity contrast in MOPITT retrievals at levels throughout the
361 vertical profile, and examines the magnitude of the difference within coastal L3 grid boxes.

362

363

364 **3.1.1. Global context**

365

366 Figure 3 shows long-term mean maps for the retrieval sensitivity metrics AK diagonal value, AK rowsum,
367 and retrieved minus a priori VMR (“VMR ret-apr”) at selected profile levels, created from L3O data averaged
368 across the entire study period (September 2001 – February 2019, inclusive). All indicators show that retrieval
369 sensitivity is greater over land than water in the lower troposphere (“LT”; represented by the surface, 900
370 hPa and 800 hPa profile levels), with sharp differences evident at almost all land-water boundaries. The
371 sensitivity contrast clearly decreases in strength with height. By mid-tropospheric levels (“MT”; represented
372 by 600 hPa profile level), AK diagonal values and rowsums reach greater values on average over water than
373 land. Some strong land-water gradients remain present in VMR ret-apr fields, most notably over North
374 Africa, the Arabian peninsula, and south-east China, but on average these values are much more similar
375 across land and water than in the LT. No clear land-water contrast is evident in the upper troposphere (“UT”;
376 represented by the 300 hPa profile level), with retrieval sensitivity instead varying more with latitude,
377 decreasing towards both poles (a companion to Fig. 3 with an altered colour bar to better show spatial patterns
378 in AK diagonal values and rowsums at MT and UT levels is provided in the Supp. Mat. (SM2)).

379 AK diagonal values and rowsums show that retrieval sensitivity increases across both land and water
380 with height. It is lowest at the surface level, with little information content in the retrieval over water (AK
381 diagonal values and rowsums over water are less than half what they are over land, on average). There is high
382 spatial variability over land: AK diagonal values and rowsums reach values comparable to those at higher
383 profile levels in some sensitivity hotspots (e.g. parts of central Europe, east Asia, eastern USA and tropical
384 west Africa), while being more comparable to values over water in other areas. By 800 hPa, AK diagonals
385 and rowsums over water reach values comparable to or greater than those reached over land at the surface
386 level, in most places.

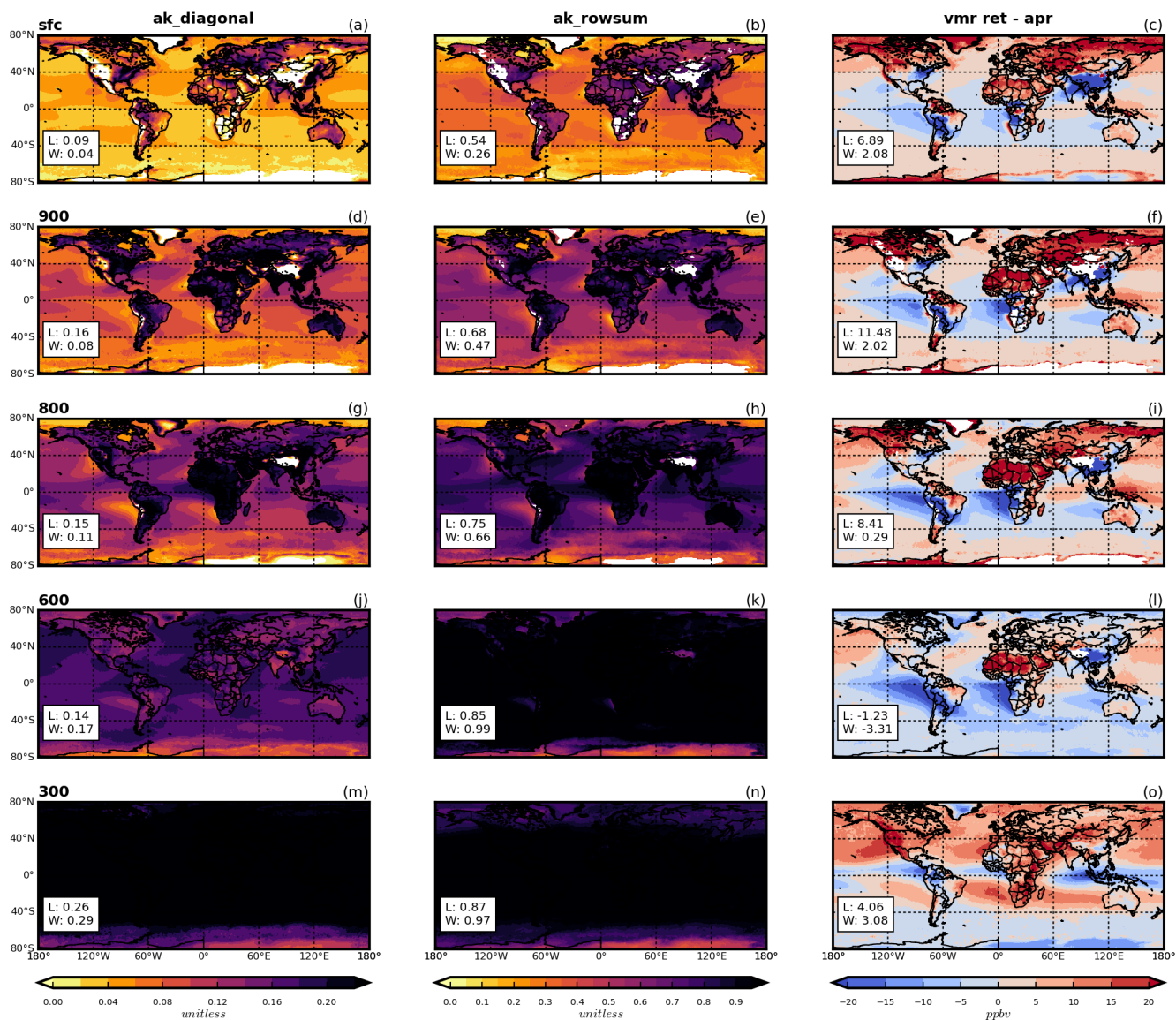


Figure 3. Mean sensitivity metrics from MOPITT L3 data, averaged across the entire study period (September 2001 – February 2019, inclusive). Shown are AK diagonal values (left column), AK rowsums (center column) and VMR retrieved minus a priori values (right column) for the following levels of the retrieved profile: surface (top row), 900 hPa (second row), 800 hPa (third row), 600 hPa (fourth row), and 300 hPa (bottom row). Values in white boxes correspond to mean values across all land (“L”) and water (“W”) L3 grid boxes.

388 Spatial patterns in retrieved minus a priori VMRs are slightly more complex to interpret, because they
389 are influenced both by retrieval sensitivity and the accuracy of the a priori. For example, while VMR ret-apr
390 values close to zero can indicate a retrieval that is heavily weighted by the a priori and therefore low retrieval
391 sensitivity, they can also indicate that the true VMR is close to the a priori value. Despite this, retrieved minus
392 a priori VMR values clearly reach more strongly positive or negative values over land than water in the LT,
393 with the contrast becoming less pronounced with height. Furthermore, there are clear land-water
394 changepoints in the LT. This further demonstrates the impact of the land-water contrast in retrieval
395 sensitivity.

396

397

398 **3.1.2. Analysis of coastal L3 grid boxes**

399

400 Scatterplots of sensitivity metrics at selected profile levels, for coastal L3 grid boxes only, are shown in Fig.
401 4. Specifically, these plots show the sensitivity of the L2 land and water retrievals that are bounded by the 1°
402 x 1° L3 grid boxes and used to create the L3O data. The values that are plotted correspond to the long-term
403 mean from the L3L and L3W datasets for these grid boxes.

404 The AK diagonal value and rowsum plots clearly demonstrate greater sensitivity over land (L3L) than
405 over water (L3W) at LT levels (a point below the diagonal line on these panels indicates greater values in
406 L3L) for the majority of grid boxes, with the difference decreasing into the MT and UT. Correspondingly,
407 retrieved VMRs also deviate more greatly from their a priori values in L3L than L3W in the LT, with smaller
408 land-water differences in the MT and UT. Mean values are significantly different ($p < 0.005$) apart from AK
409 diagonal values and retrieved minus a priori VMR at 300 hPa ($p = 0.13$ and 0.07 respectively). Sensitivity
410 metrics are generally better correlated in the MT and UT than at LT levels.

411 This analysis clearly shows how L2 retrievals that are averaged together to create the L3O data over
412 coastal grid boxes have differing degrees of sensitivity, especially in the LT. This is explicitly cautioned
413 against in the MOPITT data user's guide (MOPITT Algorithm Development Team, 2018). The remainder of
414 this paper focuses on the surface-level of the retrieved profile, since the LT is where discrepancies are
415 greatest, and the cause of this sensitivity disparity is well established: differing thermal contrast conditions
416 near to the surface over land and water; and a lack of NIR radiances being used in the retrieval over water.
417 Furthermore, the surface-level is of most interest for identifying potential air quality impacts for humans (e.g.
418 Buchholz et al., 2022).

419

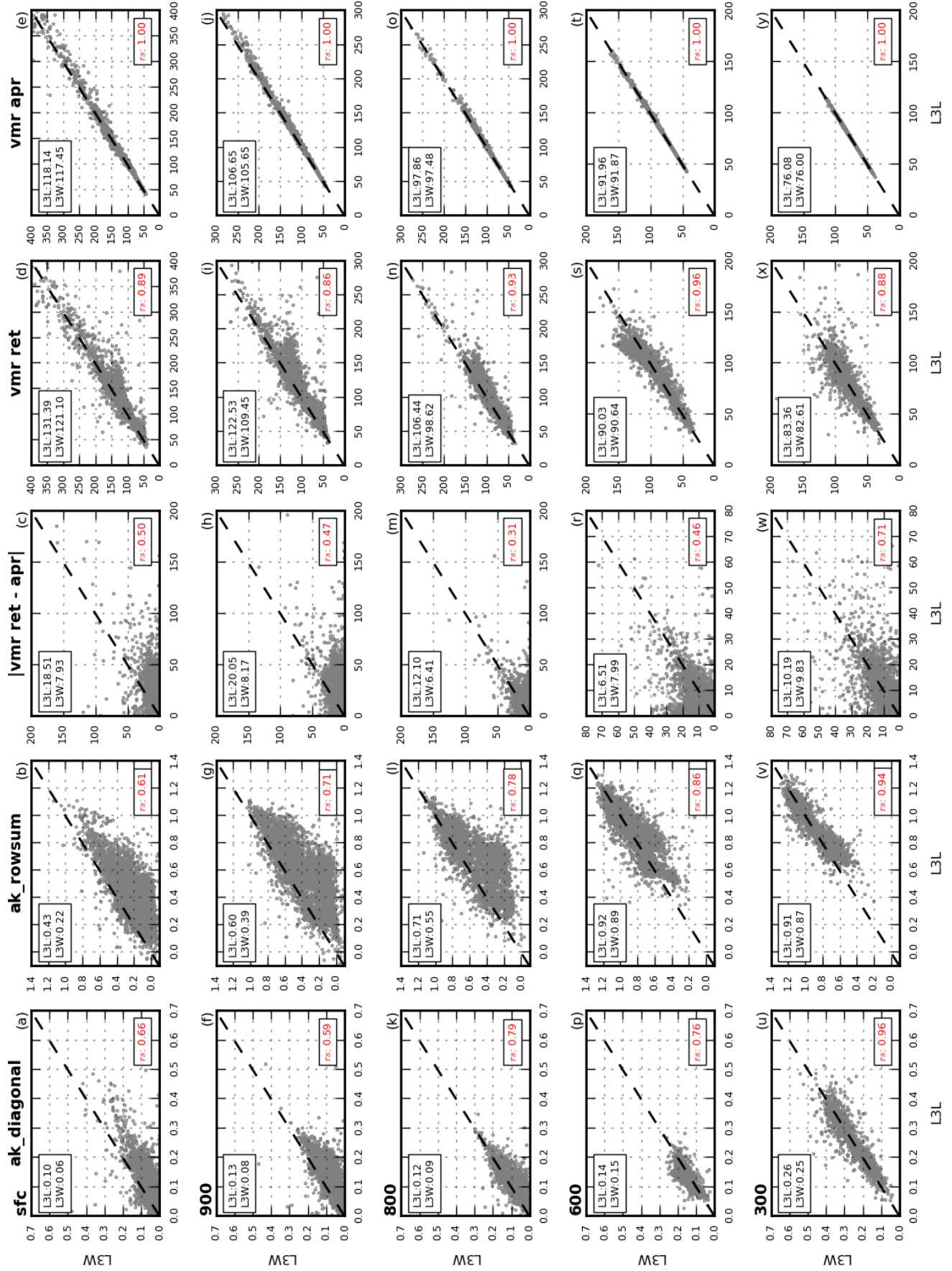


Figure 4. Mean sensitivity metrics and VMRs (retrieved and a priori) from coastal L3 grid boxes. Values compared in the scatterplots are mean values from matched L3L and L3W retrievals within these grid boxes. “Matched” means that only days when both L3L and L3W are present, and the L3O surface index is mixed, are used to create the mean values analysed. Shown are AK diagonal values (left column), AK rowsums (second column), absolute VMR retrieved minus a priori values¹ (third column), retrieved (fourth column) and a priori (fifth column) VMRs, for the following levels of the retrieved profile: surface (top row), 900 hPa (second row), 800 hPa (third row), 600 hPa (fourth row), and 300 hPa (bottom row). Values in boxes in the top-left corner of each panel correspond to mean values across all L3L and L3W grid boxes. These means are significantly different using a 2-tailed t-test (unequal variance) with $p < 0.005$ in all cases except `ak_diagonal` at 300 hPa where $p = 0.13$, `vmr_ret_minus_apr` at 300 hPa where $p = 0.07$, `vmr_ret` at 600hPa where $p = 0.30$, `vmr_ret` at 300hPa where $p = 0.11$. No `vmr_apr` mean differences are significant. Values in the bottom-right corner of each panel correspond to the Spearman’s rank correlation coefficient ($p < 0.005$ in all cases).

¹ Note that for ease of interpretation, the absolute retrieved minus a priori VMR values are plotted, i.e. ignoring whether the result is positive or negative. However, the results hold if using signed values, and a duplicate of Fig. 4 with signed retrieved minus a priori VMR values is included in the Supp. Mat. for reference (SM3).

421

422

423

424 **3.2. Differences in retrieved VMRs and temporal trends, and their relation to the land-water sensitivity**

425 **contrast**

426

427 **3.2.1. L3L vs L3W**

428

429 *Retrieved VMR comparison between L3L and L3W*

430

431 In addition to the clear land-water LT sensitivity contrast in coastal grid boxes, there are clear differences in
 432 the retrieved VMRs (Fig. 4; Fig. 5a (black boxplots)). The retrievals performed over land yield surface-level
 433 VMRs that are over 10 ppbv greater than over water, on average. As with sensitivity, land-water differences
 434 in retrieved VMRs decrease higher up in the profile.

435

436 Greater land-water sensitivity differences also tend to be associated with greater retrieved VMR
 437 differences. Figure 5b shows the distribution of retrieved surface level VMR differences ($L3L - L3W$)
 438 stratified by the corresponding surface level AK rowsum difference. Larger retrieved VMR differences are
 439 clearly associated with greater AK rowsum differences (some degree of spread in the results is expected,
 since the relationship also depends on the accuracy of the a priori, as outlined previously).

440

441 Of the 3971 coastal grid boxes that are compared, 60 % (2379) show a significant difference ($p < 0.1$,
 442 determined using a 2-tailed student’s t-test) in mean VMRs in L3L and L3W (Fig. 5a). Compared to grid
 443 boxes where the mean VMR difference is not significant, there are several notable differences (detailed in
 444 Table 1). As expected from the previous analysis, the land-water sensitivity contrast is greater when mean
 445 VMRs are significantly different (“SIGDIFF”) than when not (“NOT_SIGDIFF”). This is evident in AK
 rowsum and VMR retrieved minus a priori differences (the magnitude of difference between subsets is around

446 50 % and 100 %, respectively). Interestingly, the AK difference is due to sensitivity being lower over water
447 in SIGDIFF than in NOT_SIGDIFF; sensitivity over land is similar in both subsets. This may be explained
448 as follows: when sensitivity over water is especially low, as is the case in SIGDIFF, the retrieved VMR will
449 be heavily weighted by the a priori and unable to match the variation present in the more sensitive retrieval
450 over land. As sensitivity over water increases, this a priori weighting weakens and the retrieved VMR will
451 more closely track the retrieval over land, resulting in a less significant difference. Also of note, a priori
452 VMRs are much lower in SIGDIFF than in NOT_SIGDIFF, on average. Considered alongside the greater
453 retrieved minus a priori differences, this suggests that the a priori VMR could be a less accurate estimate of
454 the “true” VMR for the SIGDIFF subset, whereas it is closer to reality for the NOT_SIGDIFF subset.
455 Intuitively, this makes sense: for a hypothetical situation where the a priori VMR is a perfect match for the
456 “true” VMR, and both are uniform across a coastal L3 grid box, retrievals over the land and water portions
457 of the grid box would be expected to be identical irrespective of any differences in retrieval sensitivity over
458 those surfaces. To summarise: assuming “true” VMRs are similar over land and water within coastal L3 grid
459 boxes, differences in retrieved VMRs depend not only on the sensitivity of the retrieval, but also on the
460 accuracy of a priori VMRs used in the retrievals.

461 It should be noted that there are additional physical factors that could plausibly play a role in
462 generating the L3L – L3W retrieved VMR difference that is observed, in addition to retrieval sensitivity.
463 Given that most CO sources are land-based, a decrease in VMRs from land to water might be expected,
464 especially in the LT. However, this assumption only seems reasonable where large CO sources are proximal
465 to the coastline, as it is unrealistic to expect gradients as large as we observe in background CO (which coastal
466 grid boxes far from large CO sources are more likely to represent) across the relatively small distance covered
467 by a L3 grid box. Given the relatively long-lived, well-mixed nature of atmospheric CO, VMRs retrieved at
468 a given location are a function of both local emissions *and* transport, and the portion of coastal L3 grid boxes
469 situated over water therefore do not represent pristine conditions in comparison to the adjacent land-based
470 portion of the grid boxes. This is verified by comparing a priori VMRs (also shown in Figure 4), which
471 suggest the land-water difference in CO concentrations should be negligible (mean L3L – L3W a priori VMR
472 difference = 0.69 ppbv, compared to a mean retrieved VMR difference of 10.29 ppbv). The above reasoning
473 can also be applied to the question of whether wind direction is responsible for creating the observed L3L –
474 L3W difference in retrieved VMRs: It could be hypothesised that a prevailing onshore wind may lead to CO
475 concentrations being higher over land than water, yet the negligible L3L – L3W a priori VMR difference,
476 the fact that atmospheric CO is well-mixed, and the clear land-water sensitivity gradient that has been
477 demonstrated suggest that wind direction does not play a big role in creating the land-water difference
478 observed in retrieved VMRs. To further rule out the role of wind direction, the L3L – L3W retrieved VMR

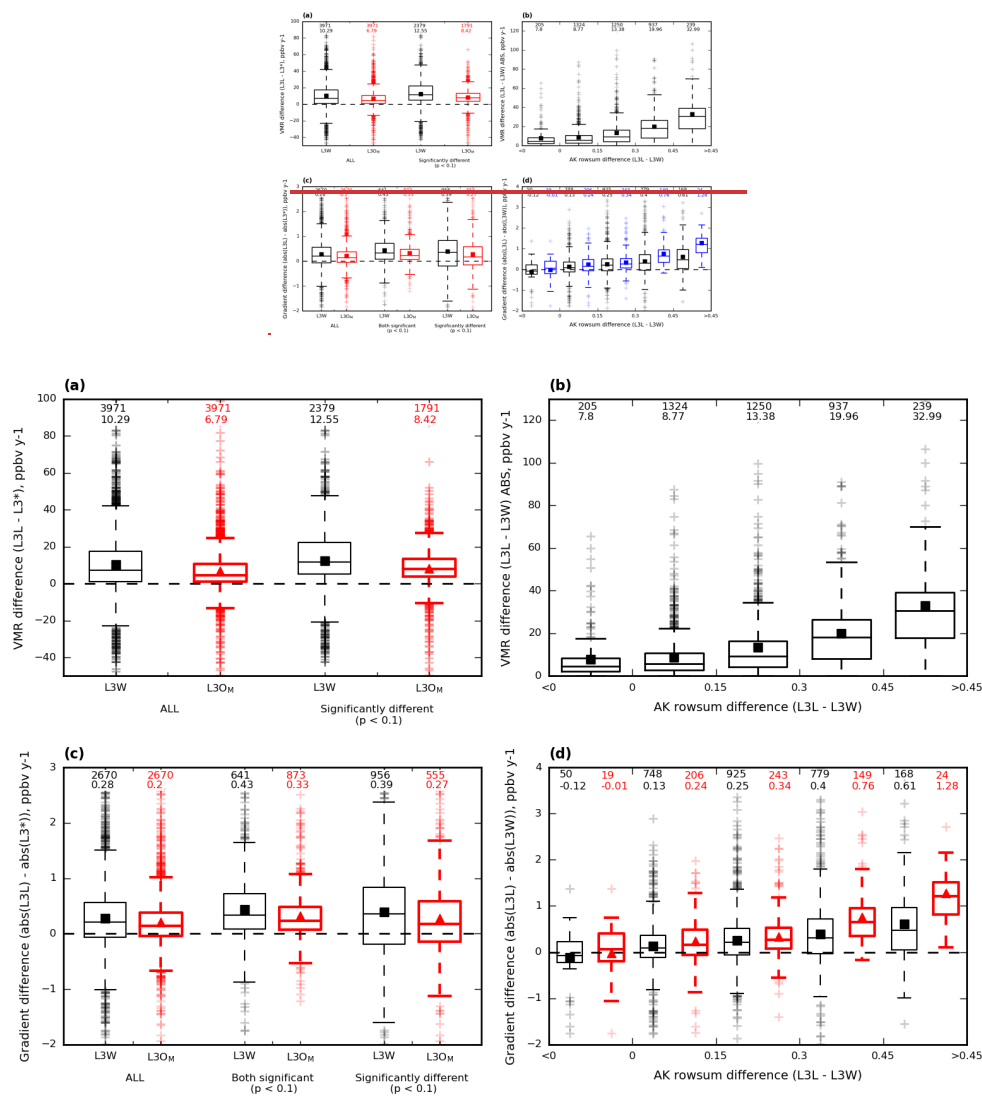


Figure 5. Boxplots showing how mean VMRs and trends from WLS analysis compare for coastal L3 grid boxes, calculated from matched retrievals within these grid boxes. “Matched” means that only days when both L3L and L3W are present and the L3O surface index is mixed are used to create the mean values analysed. Mean values are represented by filled squares/triangles, and values above the boxplots correspond to number of grid boxes with data for that boxplot, and the mean value, respectively. **(a)** Mean VMR differences for L3W (black, mean values represented by filled squares) and L3O_M (red, thicker lines, mean values represented by filled triangles) compared to L3L (L3L – L3* in both cases). Shown are the differences for all coastal grid boxes, and only for those grid boxes where the difference is significant ($p < 0.1$), determined using a 2-tailed t-test. **(b)** Absolute mean VMR differences¹ between L3L and L3W, stratified according to corresponding AK rowsum difference (L3L – L3W in both cases). **(c)** Absolute differences in gradients² detected using WLS regression analysis for L3W (black, mean values represented by filled squares) and L3O_M (red, thicker lines, mean values represented by filled triangles), compared to L3L (L3L – L3* in both cases). Shown are differences for all coastal grid boxes where WLS analysis could be performed, for grid boxes where both trends compared are significantly different to zero ($p < 0.1$), and for grid boxes where the trend difference is significant ($p < 0.1$). **(d)** Absolute differences in gradients² detected using WLS regression analysis between L3L and L3W, stratified according to corresponding AK rowsum difference (L3L – L3W in both cases). Shown are the differences for all coastal grid boxes where WLS could be performed (black, mean values represented by filled squares), and only for those grid boxes where the detected trend is significant ($p < 0.1$) in both L3L and L3W (black/red, thicker lines, mean values represented by filled triangles).

¹Absolute retrieved VMR difference values are shown in Fig. 5b for clarity, since L3L – L3W can be either positive or negative depending on whether a priori VMRs used in the retrieval are greater or less than the “true” VMR being retrieved, which complicates the analysis. The corresponding plot with raw values (i.e. not discarding the +/- sign) is included in the Supp. Mat. however, and the same conclusions can be drawn based on this figure (SM4).

²For clarity, differences between the absolute trend values (i.e. ignoring the +/- sign of the trend) are presented, since this shows the degree of difference in the trend magnitude, irrespective of trend direction. A positive trend difference in this case signifies a stronger (faster) trend in L3L than L3* (panel c) or L3W (panel d).

Table 1. Mean values for selected variables from L3L and L3W for coastal L3 grid boxes, matched retrievals only. “Matched” means that only days when both L3L and L3W are present and the L3O surface index are mixed are used to create the mean values analysed. Mean values are calculated and presented separately according to the results of a 2-tailed student’s t-test (unequal variance) performed on mean retrieved VMR values in L3L and L3W (n = 3971). Mean L3L – L3W differences are also shown for each subset (‘L-W’)

	P < 0.1 (“SIGDIFF”) (n=2379, 60 %)			P > 0.1 (“NOT_SIGDIFF”) (n=1592, 40 %)		
	L3L	L3W	L-W	L3L	L3W	L-W
Mean vmr_ret	129.97	117.41	12.55	133.52	126.60	6.90
Mean vmr_apr	113.78	113.18	0.61	124.65	123.83	0.83
Mean ret-apr	16.18	4.24	11.94	8.87	2.77	6.09
Mean ak rowsum	0.43	0.18	0.24	0.44	0.27	0.16

480 comparison has been analysed alongside wind direction for several case study grid boxes, and there appears
 481 to be no notable shift in wind direction whether L3L or L3W is greater for a given grid box. Results for this
 482 analysis are given in the Supp. Mat. (SM5). The weight of evidence therefore points towards L3L – L3W
 483 retrieved VMR differences being a function of reduced retrieval sensitivity over water compared to land.

484

485 *Trend comparison between L3L and L3W*

486

487 We now compare temporal trends detected in L3L and L3W for coastal grid boxes, and relate differences to
 488 the land-water sensitivity contrast outlined previously.

489 On average, across all grid boxes where WLS can be performed in both datasets following the criteria
 490 outlined in Sect. 2.5 (n = 2670), trends are stronger in L3L than L3W (Fig. 5c (black boxplots)), with the
 491 range of differences around 2.5 ppbv y⁻¹ (~-1 ppbv y⁻¹ to 1.5 ppbv y⁻¹). When the comparison is restricted to
 492 grid boxes where both trends are significantly different to zero (p < 0.1; 641 of the 2670 grid boxes, 24 %),
 493 a greater proportion of those grid boxes have a stronger trend in L3L than L3W (> 75%), but the overall
 494 range of differences doesn’t shift by much. The L3L – L3W trend difference is significant in 956 of the 2670

495 coastal grid boxes for which the analysis can be performed (36 %), with the range in differences spanning
496 around 4 ppbv y⁻¹. The trends are negative at 75 % of coastal grid boxes in both datasets, this value increasing
497 to 95% when the trend in both L3L and L3W is significant. Descriptive stats corresponding to the trends
498 values compared are detailed in Table 2).

499 To determine whether differences in trend can be linked to differences in retrieval sensitivity, L3L –
500 L3W trend are stratified by L3L – L3W surface level AK rowsum differences (Fig. 5d). As with mean VMR
501 differences, the size of the trend difference tends to increase as the difference in AK rowsums increases. In
502 addition, as the magnitude of AK rowsum difference increases in the positive direction (i.e. increasingly
503 greater sensitivity over land), a greater proportion of trend differences are positive (i.e. a stronger trend over
504 land). This pattern is even more pronounced when restricted to grid boxes where both trends are significant
505 (also shown in Fig. 5d).

506 In summary, these results show a general tendency for trend underestimation in surface level retrievals
507 over water compared to retrievals over land in the same coastal grid boxes obtained at the same times, which
508 appears to be linked to differences in retrieval sensitivity. The relationships found in these analyses are not
509 perfect because trend differences are sensitive to several other factors, in addition to differences in retrieval
510 sensitivity. For example, a greater trend difference would be evident if the rate of change in “true” CO
511 concentrations is faster than if it is slow/negligible, for a given sensitivity difference. Similarly, there should
512 be zero trend difference if “true” CO concentration levels are stable over time, irrespective of the magnitude
513 of difference in retrieval sensitivity. The accuracy of the a priori is a further complicating factor. An
514 underlying assumption is also that the temporal trend in “true” VMRs should not vary much across a 1° x 1°
515 L3 grid box. Hedelius et al. (2021) lends credence to this assumption with the finding that CO trends are
516 similar within regions spanning a few thousand kilometres (L3 grid boxes are ~ 100 km²), and that trends
517 within urban areas are generally indistinguishable from the trend of the broader region encompassing the
518 urban area, despite an expectation that urban trends should exceed the regional background due to a
519 concentration of CO emission sources here.

520
521
522
523
524
525
526

Table 2. Descriptive stats corresponding to the WLS trends detected in L3L, L3W, and L3O_M that are compared in the boxplots of Fig. 5c.

			Mean	Std	Median	IQR
All	L3L – L3W (n = 2670)	L3L	-0.55	1.27	-0.47	1.00
		L3W	-0.49	1.08	-0.34	0.65
	L3L – L3O _M (n = 2670)	L3L	-0.55	1.27	-0.47	1.00
		L3O _M	-0.51	1.03	-0.38	0.73
Both significant (p < 0.1)	L3L – L3W (n = 641)	L3L	-1.39	1.66	-1.15	1.08
		L3W	-1.06	1.56	-0.78	0.92
	L3L – L3O _M (n = 873)	L3L	-1.24	1.64	-1.06	1.07
		L3O _M	-1.02	1.38	-0.83	0.88
Significantly different (p < 0.1)	L3L – L3W (n = 956)	L3L	-0.64	1.39	-0.65	0.92
		L3W	-0.52	1.06	-0.43	0.67
	L3L – L3O _M (n = 555)	L3L	-0.69	1.36	-0.67	0.85
		L3O _M	-0.60	1.00	-0.51	0.68

528

529 3.2.2. Consequences for L3O data with a surface index of mixed (“L3O_M”)

530

531 To recap, L3O data are given the surface index “mixed” when neither land nor water is the dominant surface
532 type of the bounded L2 retrievals, for a given retrieval time. When this is the case, the retrievals over land
533 and water are averaged together. Users of L3O data do not have the option of choosing to only analyse the
534 subset of retrievals made over land (L3L) or water (L3W), as was done in the preceding analysis. To do so

535

536 requires the original L2 retrievals. In this section, the L3O_M retrievals are compared to the L3L retrievals that
537 were analysed in the previous section. The aim here is to demonstrate how, for some L3 grid boxes,
538 information on “true” VMRs and temporal trends that is available in the L2 retrievals over land (L3L) is
539 effectively lost to users of L3O data by their averaging together with the less sensitive L2 retrievals over
540 water (L3W).

541

543

544 For long-term mean VMRs, L3O_M unsurprisingly represents a mid-point between L3L and L3W, with lower
 545 VMRs than L3L, but a smaller difference range overall than L3W (Fig. 5a, red boxplots). The L3L – L3O_M
 546 differences in long-term mean VMR are significant at 45 % (1791) of coastal grid boxes. All but 3 of these
 547 grid boxes also see a significant difference between long-term mean VMRs in L3L and L3W. This makes
 548 sense: retrievals in L3L would not be expected to differ significantly from those in L3O_M if they do not also
 549 differ significantly from L3W. In total, 75 % of grid boxes that feature a significant difference between L3L
 550 and L3W also see a corresponding significant difference between L3L and L3O_M. There are several notable
 551 differences between this subset of coastal grid boxes (“BOTH”), compared to those that see a significant
 552 difference between L3L – L3W but not between L3L and L3O_M (“L3L_L3W_ONLY”), detailed in Table 3a:

553

- 554 • The grid boxes of BOTH see greater retrieved VMR differences between L3L and L3W than the grid
 555 box subset of L3L_L3W_ONLY (mean L3L – L3W difference of 13.84 vs 8.67 ppbv). This is logical:
 556 L3O_M only differs significantly from L3L if the underlying L3L – L3W difference is sufficiently large
 557 to persist through averaging.
- 558 • The grid boxes of BOTH also feature a greater land-water sensitivity contrast than those of
 559 L3L_L3W_ONLY. This is indicated both by L3L – L3W AK rowsum differences, driven
 560 predominantly by decreased sensitivity over water in BOTH; and by L3L – L3W retrieved minus a
 561 priori VMR differences.
- 562 • The grid boxes of BOTH tend to have a greater proportion of their surface covered by water than land
 563 when compared to L3L_L3W_ONLY. This is [determined by analysis of ratio\(land/water\) values for](#)
 564 [each grid box \(derivation of this metric is outlined in Sect. 2.4\).](#) ~~quantified by comparing the mean~~
 565 ~~number of L2 retrievals over land and water that are averaged together to make L3L and L3W each~~
 566 ~~day (“n_ret(L3L)” and “n_ret(L3W)”)~~, for each coastal grid box compared. A mean [n_ret\(L3L/L3W\)](#)
 567 [ratio](#) [ratio\(land/water\)](#) of 0.87 for BOTH indicates a greater water influence on L3O_M than for the grid
 568 boxes of L3L_L3W_ONLY, for which a mean [ratio\(land/water\)](#) ~~n_ret(L3L/L3W)~~ ~~ratio~~ of 1.00
 569 indicates a more even land/water split. Thus, L3O_M more closely resembles L3W – which is
 570 significantly different to L3L – in BOTH than in L3L_L3W_ONLY.

571

572 It is easy to understand how each of these can lead to a L3O_M retrieval that differs significantly from the
 573 corresponding L3L retrieval. Interestingly, it is also notable that retrieved and a priori VMRs are lower in
 574 BOTH than in L3L_L3W_ONLY, and that retrieved minus a priori VMR values are greater in BOTH than

575 in L3L_L3W_ONLY. This could imply that the a priori VMRs are closer to reality for the grid boxes of
 576 L3L_L3W_ONLY than those of BOTH, however further information on “true” VMRs is required to properly
 577 assess this.

Table 3a. Descriptive stats corresponding to matched retrievals over land and water (L3L and L3W) where the long-term mean retrieved surface level VMR in L3L and L3W is significantly different ($p < 0.1$, $n = 2379$). Grid boxes are divided into two subsets depending on whether long-term mean VMRs in L3L and L3O_M are significantly different ($p < 0.1$; “BOTH”) or not ($p > 0.1$; “L3L_L3W_ONLY”). $n_ret(L3L) / (n_ret(L3W))$ = the number of L2 retrievals over land (water) used to make a retrieval in L3O_M. The metric “ratio(land/water)” indicates the relative land vs water surface coverage of a L3 grid box. A ratio(land/water) $n_ret(L3L/L3W)$ value > 1 (< 1) implies that more of the L3 grid box surface is covered by land (water).

	BOTH (n = 1788, 75 %)			L3L_L3W_ONLY (n = 591, 25 %)		
Mean $n_ret(L3L/L3W)$	0.87			1.00		
	Land	Water	L-W	Land	Water	L-W
Mean vmr_ret	127.21	113.37	13.84	138.30	129.64	8.67
Mean vmr_apr	109.11	108.62	0.49	127.94	126.96	0.98
Mean ret_apr	18.11	4.75	13.36	10.36	2.68	7.68
Mean AK rowsum	0.42	0.16	0.26	0.46	0.26	0.20

	BOTH (n = 1788, 75 %)			L3L_L3W_ONLY (n = 591, 25 %)		
Mean ratio(land/water)	0.87			1.00		
	Land	Water	L-W	Land	Water	L-W
Mean vmr_ret	127.21	113.37	13.84	138.30	129.64	8.67
Mean vmr_apr	109.11	108.62	0.49	127.94	126.96	0.98
Mean ret_apr	18.11	4.75	13.36	10.36	2.68	7.68
Mean AK rowsum	0.42	0.16	0.26	0.46	0.26	0.20

580

581 Temporal trends detected in L3O_M are now compared to those in L3L (Fig. 5c, red boxplots). Overall, a
582 greater number of grid boxes feature a significant trend in both L3L and L3O_M than in L3L and L3W (873
583 vs 641; 33 % vs 24 %), and fewer see a significant difference between trends (555 vs 956; 21 % vs 36 %).
584 This is to be expected, given that the L2 retrievals contributing to L3L also contribute to L3O_M. The trends
585 in L3L and L3O_M are significantly different in just under half (47 %) of the grid boxes where the trend is also
586 significantly different between L3L and L3W (“BOTH”; Table 3b). These grid boxes are clearly more water-
587 dominated than the remaining 53 % of grid boxes where the trend difference between L3L and L3W is
588 significant (“L3L_L3W_ONLY”) but the L3L – L3O_M difference is not. This is indicated by a mean
589 $\frac{n_{ret}(L3L/L3W) - ratio(land/water)}{ratio(land/water)}$ of 0.77 for BOTH vs 0.99 for L3L_L3W_ONLY. Additionally,
590 detected trends in the grid boxes of BOTH are slightly stronger, with a greater difference between L3L and
591 L3W, than for the L3L_L3W_ONLY subset. Those L3 grid boxes featuring the strongest land-water trend
592 difference are therefore most likely to also see a significant trend difference between L3L and L3O_M. Again,
593 this is logical. Unlike with the retrieved VMR comparison above, however, there are no clear differences in
594 mean retrieved or a priori VMRs, nor sensitivity metrics, between these two grid box subsets (also detailed
595 in Table 3b). However, it is not necessarily expected that there would be clear differences in these parameters
596 for this analysis, since trend magnitudes themselves are also a variable (i.e. the trend in “true” CO varies
597 across space, independent of retrieval sensitivity or CO concentration, complicating the relationships outlined
598 above).

599 Most of the grid boxes where the L3L and L3O_M trends are significantly different also feature a
600 significant difference between L3L and L3W (453 of 555; 82 %). There are no clear differences between
601 these and the remaining 18 % of grid boxes that, counter-intuitively, feature a significant difference between
602 trends in L3L and L3O_M but not between trends in L3L and L3W. However, small discrepancies are to be
603 expected for results based on statistical thresholds, especially where the variables being compared are subject
604 to multiple different factors (e.g. land-water surface cover ratio in L3O_M; land-water sensitivity contrast;
605 retrieved VMR differences; differences in the “true” CO concentration being retrieved and its change over
606 time).

Table 3b. Descriptive stats corresponding to matched retrievals over land and water (L3L and L3W) where the temporal trend detected using WLS regression analysis on yearly-mean retrieved surface level VMR in L3L and L3W is significantly different ($p < 0.1$, $n = 956$). Grid boxes are divided into two subsets depending on whether the trend in L3L is significantly different to the corresponding trend detected in L3O_M ($p < 0.1$; “BOTH”) or not ($p > 0.1$; “L3L_L3W_ONLY”). $n_ret(L3L) - (n_ret(L3W))$ = the number of L2 retrievals over land (water) used to make a retrieval in L3O_M. The metric “ratio(land/water)” indicates the relative land vs water surface coverage of a L3 grid box. A ratio(land/water) $n_ret(L3L/L3W)$ value > 1 (< 1) implies that more of the L3-grid box surface is covered by land (water).

	BOTH (n = 447, 47 %)			L3L_L3W_ONLY (n = 509, 53 %)		
Mean n_ret(L3L/L3W)	0.77			0.99		
	Land	Water	L-W	Land	Water	L-W
Mean WLS trend	-0.72	-0.58	-0.14	-0.58	-0.47	-0.11
Mean ABS WLS trend	1.18	0.76	0.42	1.04	0.68	0.35
Mean trend standard error	0.55	0.39	0.16	0.58	0.36	0.22
Mean vmr_ret	128.25	121.36	6.90	129.22	120.20	9.02
Mean vmr_apr	117.21	117.13	0.08	116.01	115.73	0.29
Mean ret-apr	11.05	4.22	6.82	13.21	4.47	8.74
Mean AK rowsum	0.46	0.22	0.25	0.44	0.20	0.24

	BOTH (n = 447, 47 %)			L3L_L3W_ONLY (n = 509, 53 %)		
Mean ratio(land/water)	0.77			0.99		
	Land	Water	L-W	Land	Water	L-W
Mean WLS trend	-0.72	-0.58	-0.14	-0.58	-0.47	-0.11
Mean ABS WLS trend	1.18	0.76	0.42	1.04	0.68	0.35
Mean trend standard error	0.55	0.39	0.16	0.58	0.36	0.22
Mean vmr_ret	128.25	121.36	6.90	129.22	120.20	9.02
Mean vmr_apr	117.21	117.13	0.08	116.01	115.73	0.29
Mean ret-apr	11.05	4.22	6.82	13.21	4.47	8.74
Mean AK rowsum	0.46	0.22	0.25	0.44	0.20	0.24

608 3.3. Implications for users of L3O data

609

610 So far, this paper has shown a clear difference in retrieval sensitivity over land and water for coastal grid
611 boxes, demonstrated how long-term VMR statistics and temporal trends calculated using these retrievals
612 (L3L and L3W) differ, and outlined consequences of averaging these retrievals together to create L3O_M. The
613 full time series of available data in L3O is now compared with L3L and L3W, without the constraint that a
614 retrieval needs to be present in both L3L and L3W for it to be included in the analysis. This replicates what
615 a user of the L3O data would do, i.e., work with all available data.

616 Users of MOPITT data are advised to restrict their analysis to retrievals performed over land. This
617 poses a quandary for users of L3O: what to do about days with a surface index of mixed? Therefore, the
618 implications of choosing to include or discard these days are also considered. In the subsequent sections, the
619 following subsets of the full L3O time series for each coastal grid box are analysed: the full L3O time series
620 with no filtering by surface index (“L3O_{NF}”); only days with a surface index of land (“L3O_L”); and days
621 where the surface index is land or mixed (“L3O_{LM}” – i.e., only days with a L3O surface index of water are
622 discarded).

623

624

625 3.3.1. Loss of available data

626

627 The guideline to only analyse retrievals performed over land results in a huge loss of data for coastal grid
628 boxes when using the L3O dataset. We quantify this by comparing the total number of days with data for
629 analysis at each coastal grid box in L3O_L (“n_days(L3O_L)”) and L3O_{NF} (“n_days(L3O_{NF})”) (Fig. 6a).
630 Strikingly, 35 % of coastal grid boxes (total coastal grid boxes = 4299) have zero days in L3O_L, and 67 %
631 have a surface classification of land less than 5 % of the time in L3O (yielding a n_days(L3O_L/L3O_{NF}) ratio
632 of 0.05 or less in Fig. 6a). Importantly, retrievals over land are made on a large proportion of these filtered
633 days; but they are either discarded altogether or averaged together with retrievals made over water to create
634 L3O_M. This point is demonstrated by comparison to the total number of days with data for analysis at coastal
635 grid boxes in L3L (“n_days(L3L)”). In contrast to a mean (median) n_days(L3O_L/L3O_{NF}) ratio of 0.08 (0.01),
636 a mean (median) n_days(L3L/L3O_{NF}) ratio of 0.44 (0.40) demonstrates the stark loss of available data. This
637 is further highlighted by the fact that over half (56%) of coastal grid boxes have at least 25 times more days
638 with retrievals made over land than are available for analysis in the L3O dataset if filtering guidelines are
639 followed (as shown by the ratio n_days(L3L/L3O_L) in Fig. 6b (~~green~~-black line)).

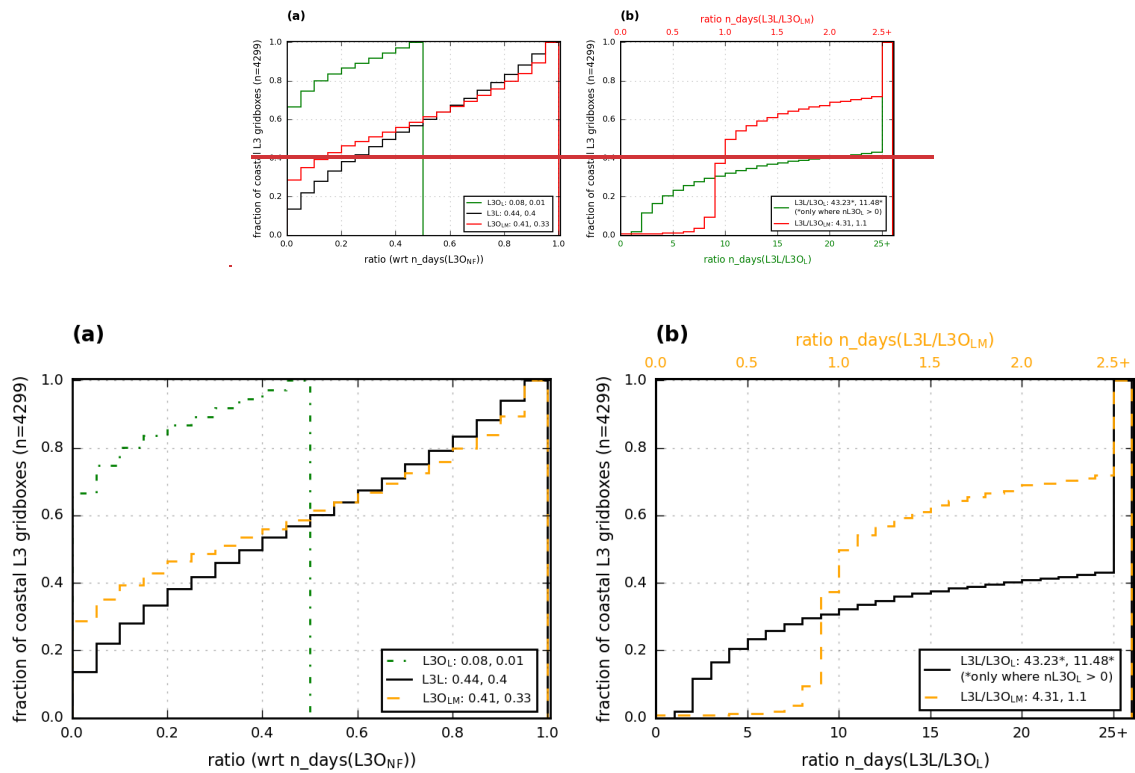


Figure 6. Cumulative frequency histograms comparing the number of days with data for different L3Osubsets and L3L at coastal L3 grid boxes. A ratio < 1 (> 1) indicates the plotted dataset has less (more) days with data than the comparison dataset that is indicated on the x-axis. **(a)** L3O_L (dash-dot green line), L3L (solid black line), and L3O_{LM} (dashed orange line) are compared to the “as-downloaded” L3O dataset, without any filtering by surface index (“L3O_{NF}”). Values in legend correspond to mean and median ratio for indicated dataset, respectively. Note, as a result of how coastal grid boxes are classified (outlined in Sect. 2.3), all $n_days(L3O_L/L3O_{NF})$ ratios are below 0.5 (i.e. at best, L3O has a surface classification of land on 50 % of days) **(b)** L3L is compared with L3O_L (green solid black line, bottom x-axis) and L3O_{LM} (red dashed orange line, top x-axis). Values in legend correspond to mean and median ratios, respectively.

641 The situation can be improved for L3O users by keeping days when the L3O surface index is classified
 642 as mixed, in addition to land (“L3O_{LM}”). Even in this best-case scenario however, L3O_{LM} sees less days with
 643 data than L3L for over 60% of coastal grid boxes ($n_days(L3L/L3O_{LM})$ in Fig. 6b (red-orange line)).
 644 Moreover, the large proportion of these L3O_{LM} days have the surface index of mixed and therefore suffer
 645 from the averaging together of retrievals over land with retrievals over water which, as has been shown, can
 646 significantly impact the results of analyses using these data. This point is returned to in following sections.

647 Intuitively, it is to be expected that the ratio $n_days(L3L/L3O_{LM})$ should *never* be < 1 . L2 retrievals
 648 over land obviously contribute to days when L3O is classified as land, and should, by definition, also
 649 contribute to days when L3O is classified as mixed. In these cases, L3L will therefore also be present.

650 However, there are two instances where L2 retrievals over land in fact do not contribute to a L3O retrieval
651 classified as mixed. Firstly, L2 retrievals themselves also have a classification of mixed, when the L2 retrieval
652 does not predominantly overlie water or land. L3O can thus have a surface classification of mixed when
653 created from bounded L2 retrievals that are either only retrieved over a mixed surface, or a combination of
654 mixed and water: in both cases, there are no L2 retrievals over land, and therefore no L3L. Secondly, analyses
655 performed for this paper identified numerous instances where L3O is classified as mixed, but the only
656 contributing L2 retrievals are retrievals over water. In these instances, L3O would therefore seem to be
657 misclassified. On days when this is the case, there will be no corresponding L3L retrieval. This is documented
658 further in the Supp. Mat. (SM6). Attempting to quantify the extent of this misclassification influence is
659 beyond the scope of this paper. In the vast majority of cases where a given grid box has a $n_days(L3L/L3O_{LM})$
660 ratio < 1 , the difference is negligible (i.e. 75 % of these grid boxes have a ratio between 0.9 and 1).
661 Irrespective, in terms of the number of days with retrievals available for analysis, L3L is an improvement
662 over $L3O_{LM}$ for more grid boxes than it is not.

663

664

665 3.3.2. Scientific implications

666

667 Long-term mean (ltm) retrieved VMR values from the different L3O subsets are compared to L3L for all
668 coastal grid boxes. As expected from the analyses in Sect. 3.2, all L3O subsets that have some influence from
669 L2 retrievals over water have a ltm retrieved VMR that is below that in L3L, on average (Fig. 7a).
670 Unsurprisingly, the closest match to L3L is $L3O_L$ (mean difference -3.1 ppbv), with the mean difference
671 increasing for each L3O subset as the influence of retrievals over water increases (e.g. $L3O_{LM}$ differs less on
672 average from L3L (mean difference = 5.2 ppbv) than $L3O_{NF}$ (mean difference = 9.1 ppbv), which additionally
673 features days when L3O is solely created from L2 retrievals performed over water).

674 Note that ltm retrieved VMRs in $L3O_L$ and L3L are not a perfect match because $L3O_L$ is only a subset
675 of L3L for each grid box considered in the analysis: L3L may be present on a day when $L3O_L$ is not owing
676 to the way that the L3O data are created (i.e., classified based on the ratio of L2 retrievals over land and
677 water, with retrievals over land potentially being discarded if these are not the majority). Apart from $L3O_L$,
678 less than 25 % of the coastal grid boxes have a retrieved ltm VMR that is greater in an L3O subset than in
679 L3L. The range of ltm differences for each of these L3O subset comparisons to L3L exceeds 35 ppbv
680 (excluding outliers), with over 25 % of coastal grid boxes compared having ltm differences exceeding 9 ppbv
681 (as indicated by boxplot upper quartile values).

682 The percentage of coastal grid boxes that feature a significant difference between ltm retrieved VMRs
 683 in L3L and each L3O subset (indicated in **red-blue** above each boxplot) is high: strikingly, it is found that,
 684 for the two subsets that L3O users could realistically choose to analyse if following data filtering guidelines
 685 (L3O_L or L3O_{LM}), almost a quarter (L3O_L) or almost half (L3O_{LM}) of coastal grid boxes see a significant
 686 difference to L3L.
 687

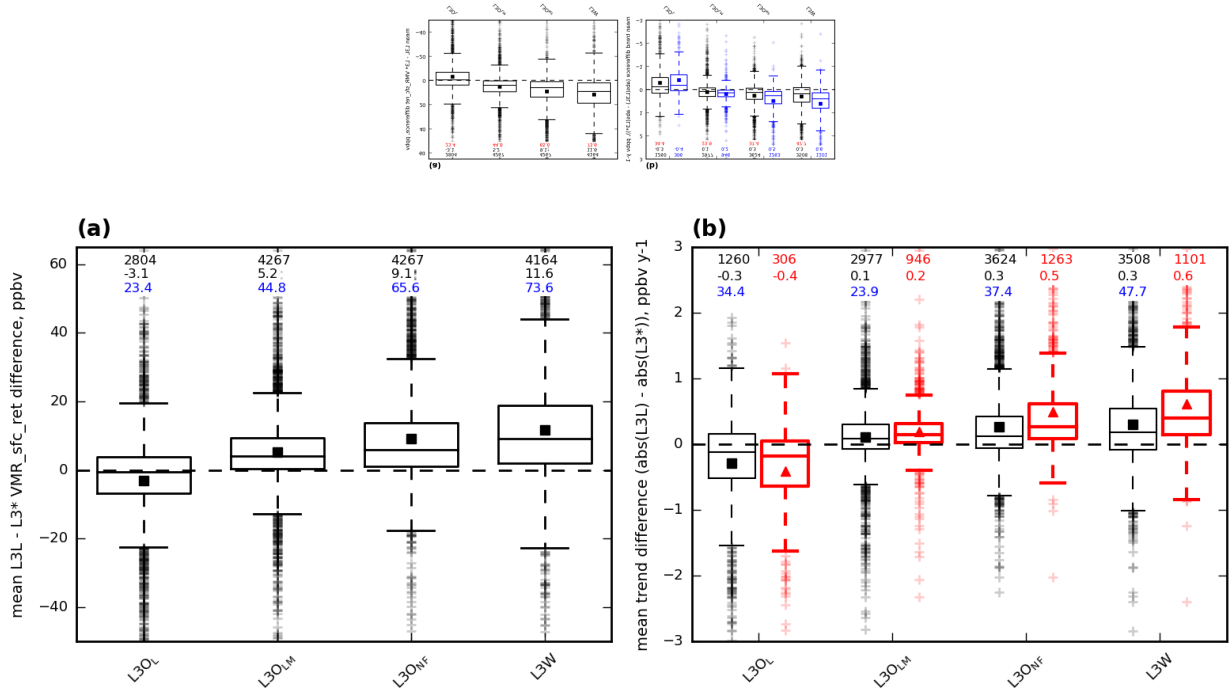


Figure 7. Boxplots showing how mean VMRs and trends compare from selected L3O subsets and L3W to L3L. Values compared are calculated from all available data across the study period. Mean values are represented by filled squares, and values above the boxplots correspond to number of grid boxes with data for that boxplot (black, top row), the mean value (black, second row), and the percentage of grid boxes represented in that boxplot that feature a significant difference with L3L (blue, third row shown in red), respectively. The comparison is calculated as L3L – L3* in both cases; therefore a point above (below) the black y=0 line indicates that the value being compared is greater (lower) in L3L. **(a)** Mean VMR differences between L3L and the indicated L3O subset or L3W. Note that the n value is different for each boxplot because not all L3 subsets are present at every coastal grid box, as shown in Sect. 3.3.1. **(b)** Differences in gradients (absolute values) detected using WLS regression analysis between L3L and the indicated L3O subset or L3W. Shown are the differences for all coastal grid boxes where WLS could be performed for both datasets compared (black, mean values represented by filled black squares), and only for the sample of those grid boxes where the detected trend is significant ($p < 0.1$) in both (red, thicker lines, mean values represented by filled triangles in blue).

688 The results of WLS regression analysis on yearly mean values from each dataset are now compared.
 689 As expected from the earlier analysis, trends are strongest, on average, in L3L and L3O_L – this is especially
 690 so when the comparison is restricted only to trends that are significantly different from zero ($p < 0.1$) (Table
 691 4). These datasets also have the largest measures of spread, indicating their tendency to yield stronger trends

692 than the other L3O subsets (and L3W), and these measures lessen for each L3O subset as the influence of
693 retrievals over water increases. Concomitant with trends decreasing in strength as the influence of retrievals
694 over water increases in each L3O subset, overall retrieval sensitivity also decreases, as indicated by the mean
695 averaging kernel metrics shown in Table 4. Comparing the magnitude of trends at each coastal grid box,
696 significant trends are stronger in L3L for at least 75% of grid boxes for all comparison datasets apart from
697 L3O_L (Fig. 7b). L3O_L sees stronger trends than L3L on average, but the comparison of these two datasets
698 needs to be interpreted with caution due to L3O_L being a subset of L3L that features far fewer days with data,
699 as discussed previously. Like with ltm retrieved VMRs discussed above, the percentage of coastal grid boxes
700 that feature a significant difference between trends detected in L3L and each L3O subset is high, with over a
701 third (almost a quarter) of the trends in L3O_L (L3O_{LM}) being significantly different to L3L.
702

Table 4. Descriptive stats corresponding to the WLS trends detected in L3L, L3W, and selected L3O subsets. Also shown are mean averaging kernel rowsums and diagonal values corresponding to the retrievals from which trends are calculated.

		L3L	L3O _L	L3O _{LM}	L3O _{NF}	L3W
Calculated from all gridboxes where WLS could be performed	Number of grid boxes	3624	1260	2999	4288	4169
	Mean (std) trend	-0.59 (1.22)	-0.52 (1.38)	-0.50 (0.95)	-0.54 (0.67)	-0.54 (0.66)
	Median (IQR) trend	-0.45 (0.89)	-0.46 (1.08)	-0.37 (0.67)	-0.42 (0.53)	-0.40 (0.54)
	Mean AK rowsum	0.45	0.45	0.33	0.28	0.22
	Mean AK diagonal value	0.10	0.10	0.08	0.07	0.06
Calculated only from gridboxes where WLS trend is significant (p < 0.1)	Number of grid boxes	1447	453	1265	2588	2499
	Mean (std) trend	-1.23 (1.55)	-1.17 (1.90)	-0.95 (1.18)	-0.79 (0.73)	-0.78 (0.72)
	Median (IQR) trend	-0.98 (0.94)	-1.09 (1.28)	-0.74 (0.75)	-0.62 (0.56)	-0.62 (0.57)
	Mean AK rowsum	0.51	0.48	0.39	0.33	0.29
	Mean AK diagonal value	0.11	0.10	0.08	0.07	0.06

703

704

705 3.4. Illustrative examples comparing L3O and L3L: analysis of the most populous coastal cities

706

707 In this section, we analyse time series from the 33 L3 coastal grid boxes that contain cities classified amongst
708 the 100 most populous in the world (derivation outlined in Sect. 2.5) to illustrate the [differences between](#)
709 [mean values and trends obtained from the L3O and L3L datasets](#). ~~potential consequences of working with the~~

710 ~~L3O dataset, compared to L3L.~~ We focus our comparison on L3O_L and L3O_{LM}, as these are the L3O subsets
711 that data users would realistically choose to analyse if following the data filtering guidelines. For clarity, ~~we~~
712 ~~from here on refer to~~ these grid boxes ~~are referred to~~ by the name of the city that they contain. A detailed case
713 study for the L3 grid box containing the city of Dubai is first presented, before considering results for all
714 cities analysed.

717 3.4.1. Detailed case study: L3 grid box containing Dubai

718
719 Summary stats derived from the L3O subsets, L3L, and L3W (included for comparison), for the L3 grid box
720 containing the city of Dubai, are given in Table 5. Figure 8 visualises the daily retrieved VMR time series
721 from L3L, with L3O_L overlaid for comparison purposes.

722 Of a possible 1620 days with data in the unfiltered L3O dataset for this grid box, a mere 70 days (4
723 %) remain for analysis when following data filtering guidelines to restricting analysis to retrievals performed
724 over land only (the L3O_L subset). By contrast, there are 1523 days available for analysis using the L3L dataset
725 for this grid box (94 % of total days with retrievals in the L3O dataset). However, in L3O, on most days these
726 retrievals over land are averaged together with retrievals over water to create L3O_M, as evidenced by the
727 L3O_{LM} subset containing 1486 days with data for this grid box (92 % of total days in the L3O dataset). That
728 L3L has a greater number of days with data than the L3O_{LM} subset indicates that there are days in L3O with
729 a surface index of water where L2 retrievals were present over land but were discarded because of the L3
730 creation process.

731 Long-term mean retrieved VMR is greatest in the land-only datasets L3O_L and L3L. The value in
732 L3O_L is 10 ppbv greater than in L3L. Given that L3O_L is a very small subset of L3L, this appears to be a
733 large overestimate, when compared to L3L. Long-term mean retrieved VMR in L3O_{LM} is 11 ppbv lower than
734 in L3L. This is clearly a result of the inclusion of retrievals over water in this dataset, via L3O_M, with long-
735 term mean retrieved VMR in L3W being 17 ppbv lower than L3L. Both the L3L vs L3O_{LM} and L3L vs L3W
736 mean differences are significant ($p < 0.1$). Consistent with the results shown in Sect. 3.2.2 when identifying
737 factors that determine whether the averaging of L2 retrievals over land and water to create L3O_M can yield
738 statistically significantly different retrievals to L3L, this L3 grid box is water-dominated, with a mean
739 ratio(land/water) of 0.60.

740 The trends detected using WLS analysis following the method outlined in Section 2.5 are visualised
741 in Figure 9 (note that trend values are also given in Table 5 in both ppbv y^{-1} and % y^{-1}), along with the yearly
742 mean VMR values that were used in the regression. Detected trends are clearly strongest in the land-only

743 datasets L3O_L and L3L, with the L3O_L trend being significantly stronger ($p < 0.1$) than the L3L trend – a
744 difference of equating almost 1 % y^{-1} (2.01 ppbv y^{-1}). Again, given the far superior temporal coverage of
745 L3L, this is the more reliable result. The trend in L3L is 0.65 % y^{-1} (1.28 ppbv y^{-1}) stronger than in L3O_{LM},
746 which corresponds to a difference of almost 12 % over the 18-year period of analysis. The trend in L3O_{LM} is
747 clearly weakened by inclusion of retrievals over water, with the trend in L3W being over 1 % y^{-1} weaker than
748 in L3L. Note that this trend analysis has been repeated using an alternative regression method which is less
749 sensitive to outlying values (Theil-Sen slope estimator), and the results are unchanged. This is detailed further
750 in the Supp. Mat. (SM7).

751 To summarise: If L3O users follow data filtering guidelines and restrict analysis to retrievals only
752 performed over land, there is a huge loss of data coverage in the L3O dataset for the coastal L3 grid box
753 containing the city of Dubai. Choosing to work with L3O_L despite this would lead to results that are clearly
754 erroneous, when compared to L3L, which has far greater temporal coverage (almost 22 times more days with
755 data than L3O_L). L3O users could make the decision to include days with a L3 surface classification of
756 “mixed” into their analysis to increase temporal coverage (the L3O_{LM} dataset analysed here). However, doing
757 so would yield both lower retrieved VMRs, on average, and significantly weaker decreasing trends, than
758 L3L. This is demonstrably due to the incorporation of retrievals over water into L3O_{LM} (via L3O_M), as shown
759 by the comparison with L3W.

Table 5. Summary stats from L3O subsets compared, L3L, and L3W (for comparison), for the L3 grid box containing the city of Dubai. Note that across the whole study period (2001-09-01 to 2018-12-31), there are 5988 MOPITT files available. There are 1620 days with data in the L3O dataset (unfiltered by surface index), 27 % of the whole study period. The WLS trend in units of $\% \text{ y}^{-1}$ is calculated by dividing the trend in units of $\text{ppbv } \text{y}^{-1}$ by the respective long-term mean VMR value.

Dataset	n days with data (% of days in L3O (n = 1620))	Long-term mean VMR (\pm standard deviation) (ppbv)	WLS trend (\pm standard error) (ppbv y^{-1})	WLS trend (\pm standard error) (% y^{-1})
L3O _L	70 (4 %)	190 (\pm 56)	-4.91 (\pm 1.21)	-2.59 (\pm 0.64)
L3O _{LM}	1486 (92 %)	169 (\pm 25)	-1.62 (\pm 0.18)	-0.96 (\pm 0.10)
L3L	1523 (94 %)	180 (\pm 44)	-2.90 (\pm 0.26)	-1.61 (\pm 0.14)
L3W	1565 (97 %)	163 (\pm 18)	-0.90 (\pm 0.13)	-0.55 (\pm 0.08)

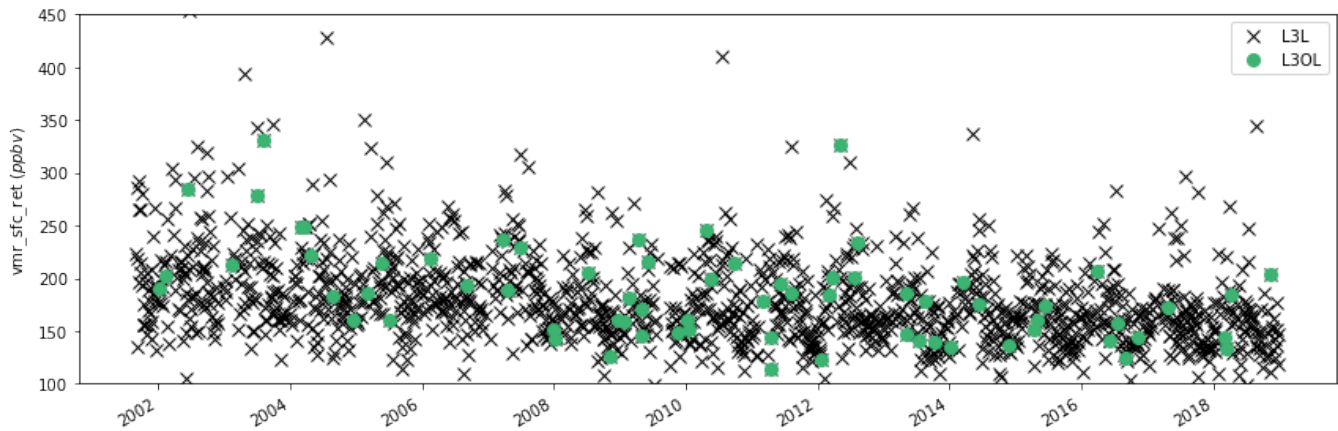


Figure 8. L3L (black crosses) and L3O_L (green circles) time series for the entire study period. Note that the size of plotted symbol required to visualise the whole time series artificially exaggerates the sense of temporal coverage; in reality, L3L is only present on 25 % of the days across the study period, and L3O_L just 1 %.

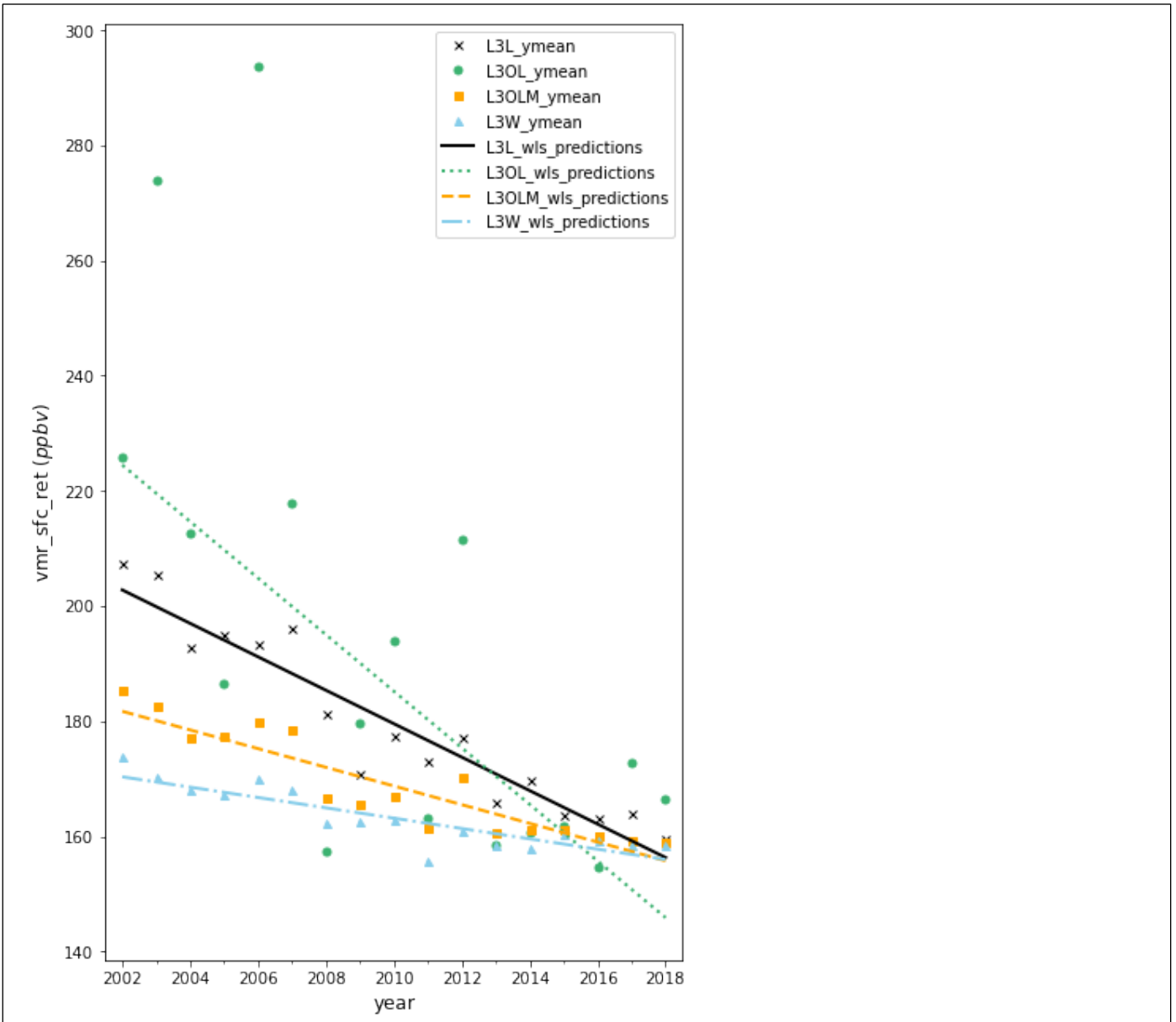


Figure 9. Yearly mean retrieved VMR in the different datasets being investigated, and the trendlines obtained from WLS regression analyses on each of these datasets. Black crosses and solid black lines correspond to L3L; green filled circles and dotted green lines correspond to L3OL; orange filled squares and dashed orange lines correspond to L3OLM; blue filled triangles and dash-dot blue lines correspond to L3W. Trend values for each dataset are also given in Table 5.

3.4.2. Discussion of results for all cities analysed

The above analysis is repeated for all cities of interest. Number of days with data, long-term mean retrieved VMRs, and temporal trends are given in Table 6 for the L3 grid boxes containing these cities for each of the L3O subsets considered, L3L, and L3W (for comparison). These metrics are evaluated in turn below.

~~3.4.1. Number of days with data~~ Temporal coverage

~~The number of days with data in L3L, L3O_L, L3O_{LM}, and L3W (included for comparison purposes) for each of the 33 L3 coastal grid boxes analysed is displayed on the right hand y-axis of Fig. 8. The loss of data in L3O if filtering for retrievals over land only (L3O_L) is clear: out retrievals over water is clear: 6 of the cities cannot be studied at all using L3O_L (number of days with data = 0), and, as there are zero days in that L3O subset. There are retrievals for all 6 in the L3O_{LM} subset, but in every case there are more days with data in L3L. Of the remaining 27 cities with data in this L3O subset L3O_L, only a single city (Osaka) has more than 50 % of the days with data in L3L-observation days. The mean n_days(L3O_L/L3L) ratio for these 27 cities is 0.189 – i.e., on average, there are over 5 times more days with data in L3L than are available in L3O when filtering for retrievals over land only. (this raises slightly to 0.23 if an additional 5 cities with only a few days (<5) of data coverage are excluded).~~

L3O_{LM} compares more favourably to L3L in terms of number of days with data, due to the inclusion of days when the L3O surface index is “mixed”, with a mean n_days(L3O_{LM}/L3L) ratio of 0.85. n_days(L3O_{LM}) > n_days(L3L) for 11 of the 33 cities, although the difference is generally small ~~ratio is less than 1.05 for all of these except San Francisco and Istanbul (ratio = 1.14 and 1.35, respectively).~~ L3O_M is the dominant component of L3O_{LM} in all cases here, being the classification on 84 % of days, on average, across all 33 cities (max = 100 %, min = 45 %).

Table 6. Summary stats for the L3 grid boxes containing the 33 cities of interest from each of the L3O subsets considered, L3L, and L3W (for comparison). For each grid box and dataset, the following stats are shown: 1. ratio(land/water), which is an indicator of the relative land vs water surface coverage of a L3 grid box; 2. the number of days with data across the whole study period; 3. the mean retrieved VMR (\pm the standard deviation), in ppbv; and 4. the trend from WLS regression analysis (\pm the standard error), in ppbv y^{-1} . Dash symbols ('-') indicate that the stat cannot be calculated for a given grid box and dataset owing to lack of data. Yellow shading indicates that a dataset mean or trend value is significantly different to the value in L3L for that city ($p < 0.1$). Grey shading indicates that the trend value is not significantly different to zero ($p < 0.1$). Diagonally striped yellow-grey shading indicates that the trend value is not significantly different to zero AND that it is significantly different to the trend in L3L for that city.

¹ The modified mean, shown in the bottom row of the table, corresponds to the mean value that is calculated only for cities where is a corresponding stat in the L3O_L dataset. For 1-3, this corresponds to cities where number of days with data L3O_L > 0 ($n = 27$). For 4, this corresponds also to cities where there are enough days with data for the regression analysis to be performed in L3O_L ($n = 18$). By contrast, the mean value, shown in the penultimate table row, simply represents the mean of all values in that column

city	1. ratio (land/water)	2. number of days with data				3. mean (\pm std) [ppbv]				4. trend (\pm standard error) [ppbv y^{-1}]			
		L3L	L3O _L	L3O _{LM}	L3W	L3L	L3O _L	L3O _{LM}	L3W	L3L	L3O _L	L3O _{LM}	L3W
Tokyo	1.57	620	98	627	575	185 (43)	188 (38)	184 (36)	178 (34)	-1.7 (0.3)	-2.3 (0.5)	-1.7 (0.3)	-1.7 (0.3)
Shanghai	1.35	378	54	374	416	373 (130)	374 (112)	363 (111)	338 (108)	-5.9 (1.4)	-7.0 (1.6)	-5.7 (1.4)	-3.4 (1.2)
Manila	0.05	127	0	86	811	150 (28)	-	151 (19)	145 (22)	-1.3 (0.5)	-	-1.2 (0.4)	-1.3 (0.2)
Mumbai	0.12	790	1	388	1356	227 (166)	291 (0)	218 (56)	184 (66)	-1.2 (0.9)	-	-0.6 (0.6)	-0.1 (0.3)
New York	0.07	216	0	178	919	296 (69)	-	315 (59)	332 (64)	-1.4 (1.1)	-	-2.3 (0.8)	-1.9 (0.5)
Lagos	0.13	116	4	92	660	337 (109)	312 (75)	305 (67)	232 (69)	1.2 (2.0)	-	0.5 (1.7)	0.2 (0.4)
Bangkok	0.52	445	33	415	755	314 (77)	346 (78)	308 (62)	261 (79)	-3.0 (0.6)	-8.6 (2.1)	-3.1 (0.7)	-2.0 (0.4)
Osaka	2.08	297	171	309	270	187 (48)	189 (39)	183 (39)	172 (34)	-2.5 (0.5)	-2.3 (0.5)	-2.3 (0.4)	-1.3 (0.4)
Karachi	1.83	1108	423	1117	884	139 (33)	130 (32)	136 (30)	131 (30)	-0.8 (0.2)	-0.6 (0.2)	-0.7 (0.2)	-0.5 (0.3)
Buenos Aires	3.05	864	241	863	719	94 (18)	95 (17)	94 (16)	95 (16)	-0.1 (0.1)	-0.5 (0.2)	-0.2 (0.1)	-0.1 (0.1)
Istanbul	0.11	322	2	436	998	152 (30)	185 (25)	154 (19)	157 (21)	-1.2 (0.4)	-	-0.4 (0.2)	-0.8 (0.2)
Chennai	0.08	331	0	95	1133	223 (56)	-	205 (25)	203 (28)	0.0 (0.8)	-	0.5 (0.5)	-0.9 (0.3)
Xiamen	0.08	215	1	97	854	263 (74)	402 (0)	258 (69)	232 (67)	-2.6 (0.9)	-	-4.1 (1.7)	-1.9 (0.4)
Taipei	0.01	36	0	5	758	192 (50)	-	210 (26)	183 (43)	-3.7 (1.0)	-	-	-1.5 (0.4)
Kuala Lumpur	0.95	142	60	143	200	233 (81)	239 (109)	234 (84)	238 (97)	-2.7 (1.3)	-3.4 (1.2)	-3.9 (1.0)	-5.1 (1.1)
Saigon	1.50	249	122	255	325	254 (65)	267 (62)	244 (60)	189 (51)	-1.4 (0.9)	-3.6 (1.3)	-2.3 (0.8)	-2.3 (0.8)
Luanda	0.67	173	54	175	341	260 (101)	312 (100)	268 (101)	213 (109)	-0.5 (2.1)	-2.6 (3.7)	0.5 (2.2)	-0.2 (1.0)
San Francisco	0.23	522	15	598	889	236 (92)	237 (67)	243 (53)	250 (60)	-1.1 (0.7)	-	-0.7 (0.5)	-1.0 (0.6)
Singapore	0.05	32	0	18	425	387 (248)	-	387 (117)	341 (133)	-	-	-	-4.3 (2.4)
Shantou	1.79	396	175	398	457	312 (96)	326 (104)	304 (91)	264 (80)	-5.4 (0.5)	-5.9 (1.4)	-5.7 (0.4)	-3.8 (0.7)
Hong Kong	0.14	228	3	164	704	336 (83)	432 (70)	312 (71)	260 (93)	-8.1 (0.9)	-	-5.1 (1.3)	-3.5 (0.5)
Toronto	2.85	401	186	416	274	238 (58)	232 (50)	239 (47)	254 (44)	-1.1 (0.8)	-0.3 (1.1)	-1.2 (0.7)	-2.0 (0.6)
Miami	0.35	411	32	357	1038	161 (32)	157 (26)	160 (25)	143 (25)	-1.5 (0.4)	-1.2 (1.2)	-1.3 (0.3)	-0.8 (0.2)
Surat	1.68	943	289	940	760	181 (44)	175 (43)	182 (43)	179 (54)	-0.4 (0.3)	-1.6 (0.7)	-0.4 (0.3)	-0.1 (0.3)
Dar Es Salaam	0.01	44	0	17	1040	103 (46)	-	86 (12)	86 (17)	-0.3 (0.7)	-	-	-0.2 (0.1)
Qingdao	2.35	587	186	589	566	372 (102)	365 (96)	370 (94)	383 (111)	-3.8 (1.5)	-2.0 (1.7)	-3.7 (1.4)	-4.2 (0.9)
Yangon	0.41	590	6	498	930	271 (70)	236 (37)	281 (66)	266 (79)	-1.5 (0.8)	-	-1.7 (0.6)	-2.1 (0.5)
Abidjan	0.48	86	38	83	349	218 (58)	232 (59)	215 (58)	156 (44)	-2.1 (1.4)	-3.6 (1.8)	-0.3 (1.4)	-0.7 (0.3)
Wenzhou	0.56	386	25	347	705	268 (75)	308 (122)	256 (65)	231 (64)	-4.2 (0.7)	-10.1 (2.4)	-3.5 (0.6)	-2.8 (0.6)
Sydney	0.38	709	6	676	1000	94 (36)	92 (17)	90 (16)	87 (15)	-0.7 (0.2)	-	-0.5 (0.1)	-0.2 (0.1)
Accra	0.17	155	7	116	740	245 (84)	262 (68)	224 (63)	161 (48)	2.9 (1.5)	-	2.9 (0.8)	-0.5 (0.3)
Dubai	0.60	1523	70	1486	1565	180 (44)	190 (56)	169 (25)	163 (18)	-2.9 (0.3)	-5.0 (1.2)	-1.6 (0.2)	-0.9 (0.1)
Chittagong	0.81	653	49	628	888	296 (66)	316 (79)	304 (66)	296 (91)	-0.7 (0.5)	-2.1 (2.2)	-0.7 (0.5)	-0.9 (0.7)
Mean	0.82	427	71	394	736	236	255	232	212	-1.9	-3.5	-1.7	-1.6
Modified mean ¹	0.99	493	87	466	712	238	255	233	212	-2.3	-3.5	-2.1	-1.8

3.4.2. VMR comparison VMR comparison

~~Mean VMRs calculated across the entire study period are shown in Fig. 8 for L3L, L3O_L, L3O_{LM}, and L3W.~~

The consequence of the loss of data in L3O_L is clear: compared to L3L, mean VMR in L3O_L is higher, and the magnitude of this difference generally depends upon how much data is lost in L3O_L. Mean VMR across all cities (excluding the 6 cities where $n_days(L3O_L) = 0$) is ~~17.2~~ ppbv higher in L3O_L than in L3L. This falls to ~~9.8-10~~ ppbv if restricted to cities where the $n_days(L3O_L/L3L)$ ratio is greater than 0.05 ($n=17$), and ~~7.6-8~~ ppbv if restricted to cities where the $n_days(L3O_L/L3L)$ ratio is above 0.2 ($n=11$). The mean VMR difference ($L3L - L3O_L$) is significant ($p < 0.1$) for 11 of the 27 cities that can be compared; in these cases, L3O_L is a smaller subset of L3L than for the cities where mean VMR difference is not significant ($n_days(L3O_L/L3L) = 0.15$ vs 0.22 , respectively), and the mean VMR difference is unsurprisingly much greater (~~-36.49~~ vs ~~-43.93~~ ppbv).

The $L3L - L3O_{LM}$ mean VMR difference is relatively small, by comparison (~~43.7~~ ppbv, all 33 cities). However, this does hide some much larger discrepancies between L3L and L3O_{LM} for certain cities, with the difference exceeding 10 ppbv in 11 cases and 20 ppbv for 3 of them. The difference is significant ($p < 0.1$; “SIGDIFF”) for 13 of 33 cities (39 %). Compared to the subset where the $L3L - L3O_{LM}$ mean difference is not significant ($n = 20$, 61 %; “NOT_SIGDIFF”), the following characteristic differences are found (also detailed in Table ~~75~~):

- The grid boxes in SIGDIFF have a greater proportion of their surface covered by water than NOT_SIGDIFF: this is evidenced by a mean ratio(land/water) of 0.51 in SIGDIFF vs 1.02 in NOT_SIGDIFF, indicating there ~~there being~~are relatively more retrievals over water than land in ~~SIGDIFF than NOT_SIGDIFF (the ratio $n_ret(L3L/L3W) = 0.51$ vs 1.02 respectively)~~the former; and also by the fact that on average, L3O_L only contributes to L3O_{LM} in SIGDIFF on 9 % of days, vs 20 % of days for NOT_SIGDIFF (which means that retrievals over water contribute via L3O_M more frequently to L3O_{LM} in SIGDIFF than NOT_SIGDIFF).
- The $L3L - L3W$ VMR_RET differences are larger in SIGDIFF than NOT_SIGDIFF (mean = 31.15 vs 18.44 ppbv), meaning they are less likely to be hidden by averaging to create L3O_M.
- ~~Although analysis of mean averaging kernels over~~Land-water mean averaging kernel differences ~~land and water~~ suggest there is not a large land-water sensitivity contrast between the SIGDIFF and NOT_SIGDIFF subsets ~~(mean $L3L - L3W$ rowsum (diagonal value) differences are 0.25 vs 0.21 (0.10 vs 0.08) for SIGDIFF and NOT_SIGDIFF cities, respectively).~~ However, the $L3L - L3W$ retr-
apr difference, which is another indicator of sensitivity difference, is much greater for SIGDIFF than

§30 NOT_SIGDIFF: (21.66 vs 3.22 ppbv, respectively (21.98 vs 11.88 ppbv if using absolute values)).
§31 There is some evidence that this may be a function of the a priori VMRs being closer to “true” VMRs
§32 in NOT_SIGDIFF, with mean retrieved minus a priori VMR values being closer to zero than in
§33 SIGDIFF. ~~L3L retrieved minus a priori VMR values fall from -19.82 ppbv for SIGDIFF to -7.07 ppbv~~
§34 ~~for NOT_SIGDIFF (39.86 ppbv and 18.79 ppbv respectively, if using absolute values). A similar~~
§35 ~~pattern is seen in L3W, although less pronounced (-14.75 and -6.73 ppbv, respectively (18.21 and~~
§36 ~~15.57 ppbv if using absolute values)).~~

837
838 These findings are all consistent with what was shown in Sect. 3.2.2 when identifying factors that
839 determine whether the averaging of L2 retrievals over land and water to create L3O_M can yield a statistically
840 significantly different retrieval to L3L. As outlined above, L3O_M is the dominant component of L3O_{LM} in all
841 cases considered here (being the classification on 84 % of days, on average (max = 100 %, min = 45 %)).

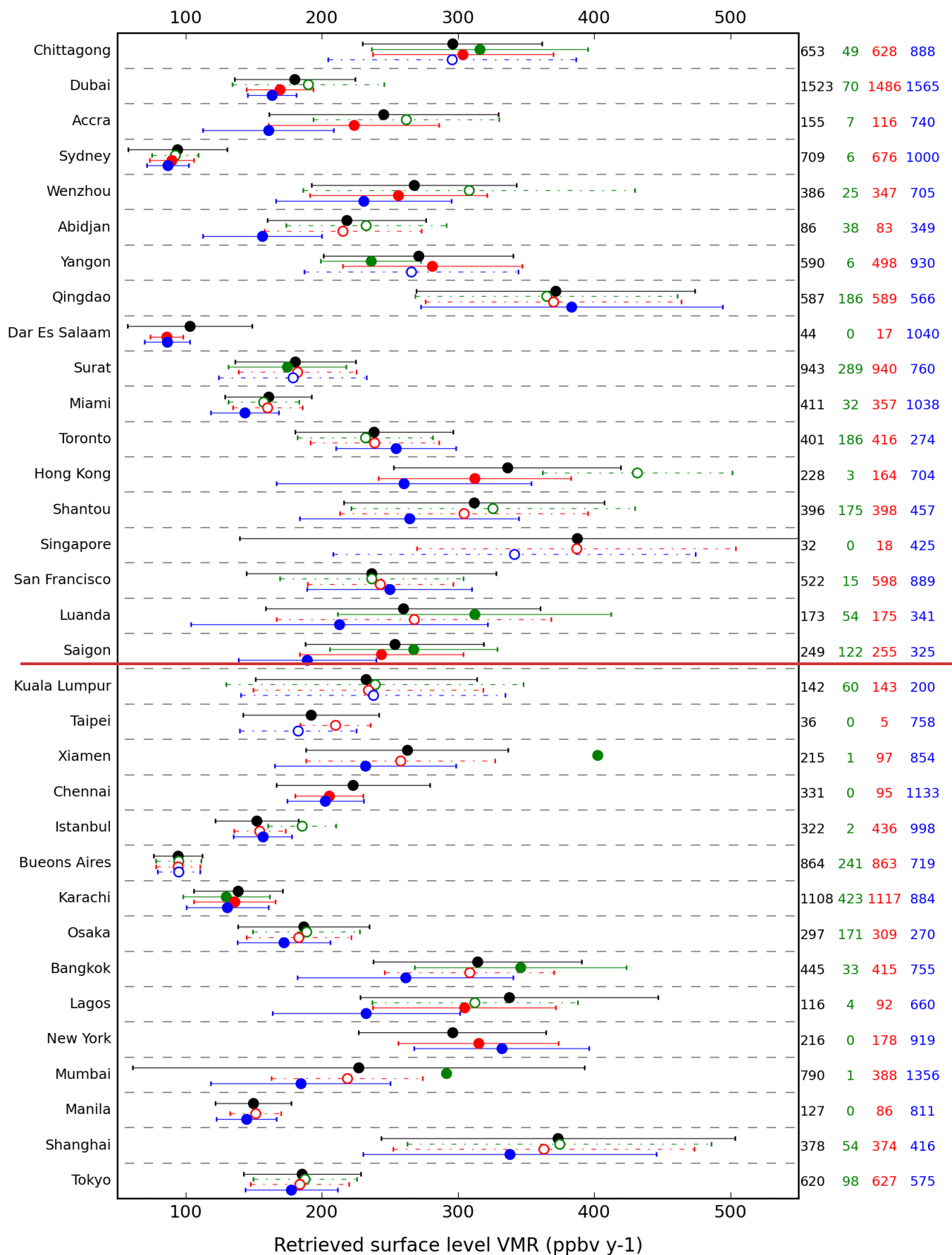


Figure 8. Comparison of long-term mean retrieved surface level VMR in L3L (black), L3O_L (green), L3O_{LM} (red), and L3W (blue), for the 33 largest coastal cities (ordered on the y-axis by population). The long-term mean value (in ppbv) is indicated by the filled/open circle on each row, and its standard deviation by the error bars. The L3L marker is always filled and lines are always solid. For other datasets, the marker style (filled/open) and line style (solid or dash/dot) indicates the significance of difference against L3L, based on an independent, 2-tailed t test assuming unequal variance (aka “Welch’s test”): filled markers and solid lines indicate the mean is significantly different to L3L ($p < 0.1$); open markers and dash/dot lines indicate there is no significant difference to L3L. The number of retrieval days in the time series analysed for each city is given on the right-hand y-axis, color-coded according to dataset.

Table 75. Selected parameters from L3 grid boxes containing cities, stratified according to whether where mean VMR in L3L and L3O_{LM} is significantly different (“SIGDIFF”; $p < 0.1$) or not (“NOT_SIGDIFF”).

	P < 0.1 (“SIGDIFF”) (n = 13)	P > 0.1 (“NOT_SIGDIFF”) (n = 20)
ratio n_ret(L3L/L3W)*	0.51	1.02
% days from L3O _L	9	20
Δ VMR_RET (L3L – L3W) (ppbv)	31.15	18.44
Δ AK rowsum (L3L – L3W)	0.25	0.21
Δ AK diagonal (L3L – L3W)	0.10	0.08
Δ VMR (RET - APR) (L3L – L3W) (ppbv)	21.66	3.22
$ \Delta$ VMR (RET - APR) (L3L – L3W) (ppbv)	21.98	11.88
L3L VMR (RET - APR)	-19.82	-7.07
$ $ L3L VMR (RET - APR) $ $	39.86	18.79
L3W VMR (RET - APR)	-14.75	-6.73
$ $ L3W VMR (RET - APR) $ $	18.21	15.57

*n_ret(L3L) (n_ret(L3W)) = the mean number of L2 retrievals over land (water) that are averaged to make a L3L (L3W) retrieval.

	P < 0.1 (“SIGDIFF”) (n = 13)	P > 0.1 (“NOT_SIGDIFF”) (n = 20)
Mean ratio(land/water)	0.51	1.02
% days from L3O _L	9	20
Δ VMR_RET (L3L – L3W) (ppbv)	31.15	18.44
Δ AK rowsum (L3L – L3W)	0.25	0.21
Δ AK diagonal (L3L – L3W)	0.10	0.08
Δ VMR (RET - APR) (L3L – L3W) (ppbv)	21.66	3.22
Δ VMR (RET - APR) (L3L – L3W) (ppbv)	21.98	11.88
L3L VMR (RET - APR)	-19.82	-7.07
L3L VMR (RET - APR)	39.86	18.79
L3W VMR (RET - APR)	-14.75	-6.73
L3W VMR (RET - APR)	18.21	15.57

848

849

850

3.4.3. Trend comparison Trend comparison

851

852

~~The above analysis is repeated with temporal trends detected using WLS regression, as outlined in Section 2.5. The trend values, their associated standard errors, and an indication of their statistical significance ($p < 0.1$) are presented for each city in Fig. 9. Where trend information is not plotted from a dataset for a given city, this means that there were too few data points to perform the regression analysis.~~

855

856

— On average, the strongest trends are seen in L3O_L. However, as with the Dubai case study, this often appears as an outlier compared to the other datasets – ~~likely~~ a consequence of theits comparatively very sparse temporal coverage ~~comparatively few L3O_L data points that the regression analysis is based on~~. As expected from previous sections, the weakest trends are detected in L3W, with L3O_{LM} representing a mid-point between this and L3L.

857

858

859

860

861

Of the 18 cities where WLS analysis can be performed in L3O_L, there are 9 where the resulting trend – and thus conclusion drawn from the analysis – is significantly different to that in L3L. In 3 of these cases (Dubai, Wenzhou, Bangkok), the trend in L3O_L can be judged to be a strong over-estimate given the large difference to the corresponding trends in L3L (trend standard errors do not overlap), and the very small number of days with data that these trends are based on when compared to L3L ($n_days(L3O_L/L3L)$ ratio < 0.08 in each case). There are 4 additional cities where a significant trend in L3O_L appears to be an over-estimate, when compared the L3L: Abidjan, Surat, Saigon, and Buenos Aires. This is because the trend for

865

866

867

868 these cities in L3L is not significantly different to 0 which, given the higher number of days with data in L3L
869 ($n_days(L3O_L/L3L)$ ratio = 0.44, 0.31, 0.49, 0.28, respectively), appears to be the more reliable result. The
870 L3O_L trend for Miami is insignificant and derived from very low n. L3O_L is also the only dataset to yield an
871 insignificant trend for Qingdao.

872 As with mean VMRs, trends in L3O_{LM} compare better than L3O_L to L3L. However, there are still 5
873 cases where L3O_{LM} and L3L yield significantly different results. For 3 of these (~~Dubai~~, Hong Kong, ~~and~~
874 Istanbul, [and Dubai, as covered in detail in Sect. 3.4.1](#)), interpretation of the difference is simple: L3O_{LM} is
875 a significant under-estimate of the CO change over time. This is very likely due to the inclusion of retrievals
876 over water in this dataset, as evidenced by L3W yielding a significantly weaker trend than L3L in all 3 cases.
877 In the remaining 2 cases – New York and Saigon – interpretation is more complicated. For both these cities,
878 the trend detected in L3L is not significantly different from zero, whereas the trend in L3O_{LM} is. Does this
879 mean that the trend in L3O_{LM} is an over-estimate? Possibly. However, in both cases, the trends are within
880 one standard error of each other and therefore within the range of sampling uncertainty. There are an
881 additional 2 cities where WLS could be performed in L3L but not L3O_{LM} (Dar Es Salaam and Taipei), but
882 $n_days(L3L)$ is so low (44 and 36, respectively) that these results are not deemed to be trustworthy.

883 As outlined in Sect. 2.5, it is important to note that the trends presented in this section are for
884 illustratory purposes only, with the intention of demonstrating that different results can be obtained depending
885 on whether L3O or L3L (and, by extension, L2) data are analysed. More focused analysis is needed to verify
886 these trends, which is beyond the scope of this paper. [The trend analysis has been repeated using an alternative
887 regression method which is less sensitive to outlying values \(Theil-Sen slope estimator\), and the main results
888 reported above stand. This is detailed further in the Supp. Mat. \(SM7\).](#)

889

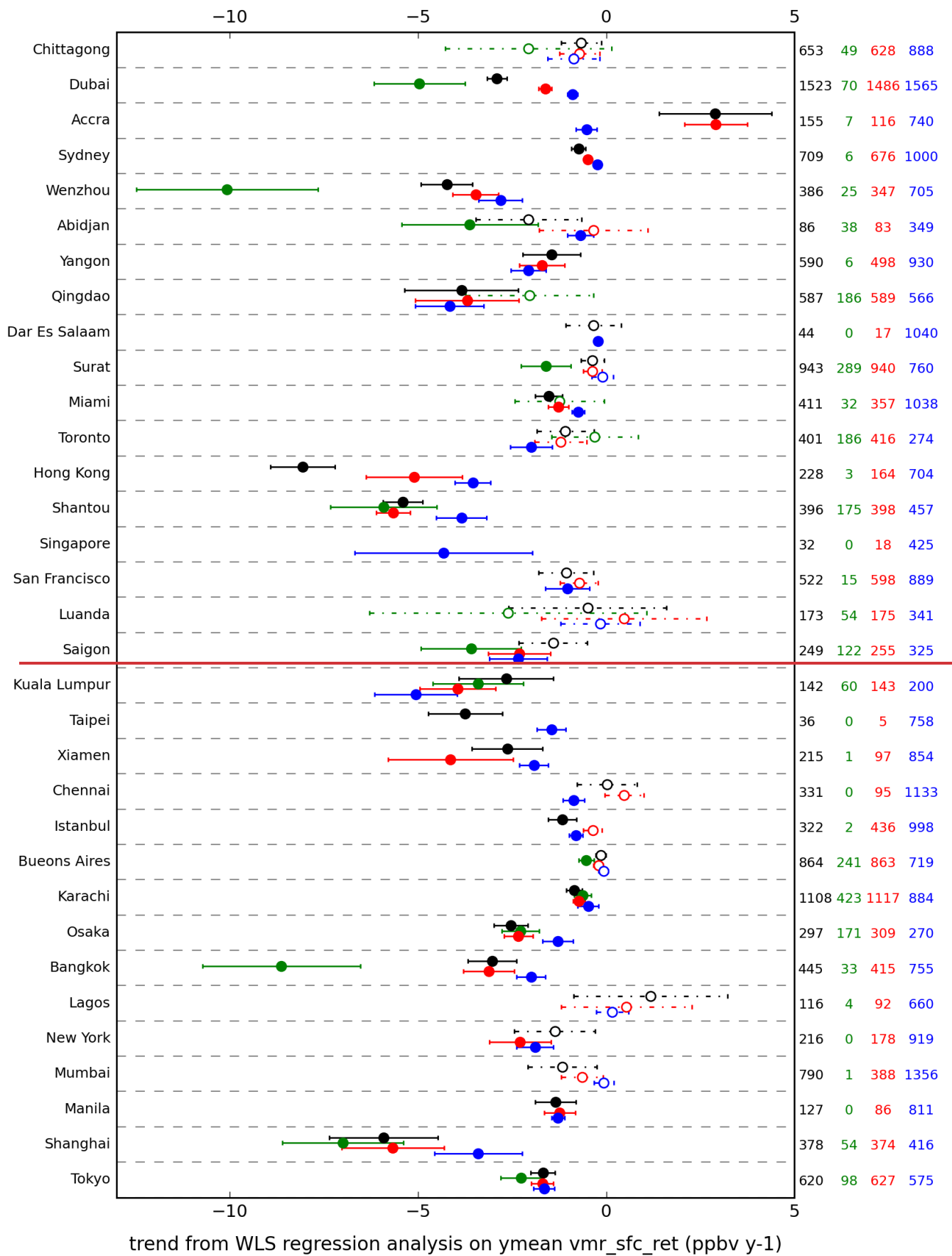


Figure 9. Comparison of temporal trend (detected using WLS, as outlined in Section 2.5) in retrieved surface level VMR in L3L (black), L3O_L (green), L3O_{LM} (red), and L3W (blue), for the 33 largest coastal cities (ordered on the y axis by population). The trend value (in ppbv y⁻¹) is indicated by the filled/open circle on each row, and its standard error by the error bars. For all datasets, whether the marker is filled or not, and whether the lines are solid or dash/dot, depends on the significance of the trend: filled markers and solid lines indicate the trend is significant ($p < 0.1$); open markers and dash/dot lines indicate that the trend is not significantly different to zero. The number of retrieval days in the time series analysed for each city is given on the right hand y axis, color coded accorded to dataset.

4. Summary and Conclusions

Motivated by the work of Ashpole and Wiacek (2020) which demonstrated, for the MOPITT L3 grid box containing the coastal city of Halifax, Canada, that mean VMR statistics and temporal trends differ depending on whether L2 or L3 data are analysed, this paper has examined what proportion of all coastal L3 grid boxes also see differences between results from analyses performed with L2 and L3 data. While it is recommended to MOPITT data users that analyses are restricted to retrievals performed over land owing to known sensitivity issues over water (MOPITT Algorithm Development Team, 2018; Deeter et al., 2015), such recommendations cannot practically be followed by users of L3 data for coastal grid boxes owing to the way the data are created from their bounded L2 retrievals. In short, this study has sought to answer the question: “does it matter”? [Analysis has focussed on comparing the original, “as-downloaded” L3 dataset \(“L3O”\) with new land-only and water-only L3 products \(“L3L” and “L3W” respectively\) that have been created from the L2 retrievals.](#) The main results are summarised below.

First, a direct comparison of the L2 retrievals performed over land (L3L) and water (L3W) that are averaged together to create L3 products on days when the L3 surface index is “mixed” (L3O_M) identified that:

- Retrieval information content is clearly greater in L3L than L3W. The corresponding mean L3L – L3W VMR difference is over 10 ppbv, significant ($p < 0.1$) at 60 % of the coastal grid boxes compared.
- Temporal trends are also stronger, on average, in L3L (mean diff = 0.28 ppbv y⁻¹, 0.43 ppbv y⁻¹ if only considering trends significantly different to zero), with the L3L – L3W trend difference significant ($p < 0.1$) at 36 % of grid boxes where a trend comparison was possible.

- Larger L3L – L3W differences in mean VMRs and trends are clearly associated with greater differences in retrieval sensitivity.
- The resulting VMRs in L3O_M are significantly different to L3L for 75 % of grid boxes where the L3L – L3W difference is also significant; this corresponds to 45 % of all coastal grid boxes compared. Whether or not L3O_M and L3L differ significantly depends on multiple factors including the ratio of land/water surface cover in the grid box, the strength of the land-water sensitivity contrast and VMR difference, and, potentially, the accuracy of the a priori.
- Just under half of the grid boxes that featured a significant L3L – L3W trend difference also see trends differing significantly between L3L and L3O_M. As with the mean VMR comparison, these grid boxes are more water-dominated than the subset whereby the L3L – L3W trend difference is significant but the L3L – L3O_M trend difference is not. They also feature stronger L3L – L3W trend differences overall, but no other variables (such as ltm VMRs and sensitivity metrics) show clear differences.

Having established the degree of difference in L3O_M and L3L retrievals that is caused directly by averaging L3L with the less-sensitive L3W, the full L3O dataset with differing surface filtering options was compared to L3L:

- If L3O is filtered so that only retrievals over land (L3O_L) are analysed, as has been recommended (MOPITT Algorithm Development Team, 2018; Deeter et al., 2015), there is a huge loss of data, in terms of days with data to analyse. This is a direct result of L2 retrievals over land routinely being discarded during the L3O creation process, or averaged with L2 retrievals over water, creating L3O_M (at least for coastal grid boxes). The problem can be alleviated by also retaining L3O_M retrievals, but these additional days with data feature some influence from retrievals made over water that can affect results, as outlined. The resulting L3O_{LM} subset still has less days with data than in L3L for 61 % of coastal grid boxes.
- Almost a quarter (half) of coastal grid boxes see a significant difference in ltm VMR between L3L and L3O_L (L3O_{LM}). Over a third (almost a quarter) of the trends in L3O_L (L3O_{LM}) are significantly different to L3L.
- Focusing on the L3 grid boxes containing the 33 largest coastal cities in the world, mean VMRs in L3O_L and L3L differ significantly for 11 of the 27 grid boxes that can be compared (40 %; there are no L3O_L data for the remaining 6 cities). The L3L – L3O_{LM} mean VMR difference across all 33 grid boxes is relatively small (3.7 ppbv), but this does hide some much larger discrepancies, with the

948 difference exceeding 10 ppbv for 11 of the 33 grid boxes and 20 ppbv for 3 of them. The difference
949 is significant for 13 of 33 grid boxes (39 %). Of the 18 grid boxes where WLS analysis can be
950 performed in L3O_L, there are 9 cases where the trend is significantly different to that in L3L. The
951 trends in L3O_{LM} and L3L differ significantly for 5 of the 33 grid boxes.

952
953 From these results, it can be concluded that, yes, for at least a quarter of all MOPITT coastal L3 grid
954 boxes, it does matter that there is limited capacity to filter out the influence of retrievals over water in L3
955 data – at least without a huge loss of temporal coverage. Demonstrably, there are significant differences in
956 the mean VMRs and temporal trends that can be obtained using L3O and L3L, sometimes very large. These
957 differences could have tangible consequences, depending on the purpose for which the MOPITT data are
958 being used. While acknowledging that this analysis has also shown that there is a sizeable proportion of
959 coastal grid boxes where statistically, mean VMRs and trends do not differ significantly between L3L and
960 L3O, there is enough evidence to support the suggestion from Ashpole and Wiacek (2020) that an additional
961 L3 “land-only” product, created only from averaging bounded L2 retrievals performed over land – the L3L
962 dataset that has been analysed in this paper – ~~wc~~ could be beneficial to the research community. This dataset
963 ~~would~~ enables L3 users to maximize retrieval information content for coastal L3 grid boxes, as is currently
964 only possible with L2 data, while also preserving the benefits of L3 products, such as smaller file size and
965 greater accessibility of gridded products. [The L3L dataset analysed in this paper is publicly available for
966 download \(Ashpole and Wiacek, 2022; L3W is also available\).](#) Although this paper has focused only on
967 analysis of MOPITT data, it is reasonable to question whether the findings are applicable to data products
968 from other satellite instruments that make CO retrievals based on observed thermal-infrared radiances, such
969 as AIRS (Atmospheric InfraRed Sounder), TES (Tropospheric Emission Spectrometer), and IASI (Infrared
970 Atmospheric Sounding Interferometer).

976 **Data availability**

977

978 [The “L3L” and “L3W” datasets analysed in this study are available from the following link:](#)
979 <https://doi.org/10.5683/SP3/ERCG2H> (see also Ashpole and Wiacek, 2022). Code for creating these datasets
980 [is available here: https://github.com/ianashpole/MOPITT_L3L_L3W](https://github.com/ianashpole/MOPITT_L3L_L3W). The MOPITT V8 joint TIR-NIR files
981 [Level 2 \(“MOP02J”\) and Level 3 \(“MOP03J”\) datasets can be accessed from the following URLs,](#)
982 [respectively: https://doi.org/10.5067/TERRA/MOPITT/MOP02J_L2.008](https://doi.org/10.5067/TERRA/MOPITT/MOP02J_L2.008) (NASA/LARC/SD/ASDC, 2000a)
983 [and https://doi.org/10.5067/TERRA/MOPITT/MOP03J_L3.008](https://doi.org/10.5067/TERRA/MOPITT/MOP03J_L3.008) (NASA/LARC/SD/ASDC, 2000b) ~~were~~
984 ~~downloaded from the NASA Earthdata portal (<https://search.earthdata.nasa.gov/>).~~ ~~The L3L and L3W~~
985 ~~products analysed in this study are available on request from the corresponding author.~~

986

987

988

989 **Author contributions**

990

991 IA and AW jointly conceived of and designed the study. IA performed data analysis; both authors examined
992 and interpreted the results, and prepared the manuscript.

993

994

995 **Competing interests**

996

997 The authors declare that they have no conflict of interest.

998

999

1000 **Acknowledgements**

1001

1002 The authors received funding from the Canadian Space Agency through the Earth System Science Data
1003 Analyses program (grant no. 16SUASMPTN), the Canadian National Science and Engineering Research
1004 Council through the Discovery Grants Program, and Saint Mary’s University. We thank the MOPITT team
1005 for providing the data used in this study. The authors would also like to thank two anonymous reviewers [and](#)
1006 [the associate editor](#) whose thoughtful comments helped to improve this manuscript.

1007

1008

1009
1010
1011
1012
1013
1014
1015
1016 **References**
1017

- 1018 Ashpole, I., & Wiacek, A.: Impact of land-water sensitivity contrast on MOPITT retrievals and trends over
1019 a coastal city, *Atmospheric Measurement Techniques*, 13(7), 3521–3542, [https://doi.org/10.5194/amt-13-](https://doi.org/10.5194/amt-13-3521-2020)
1020 [3521-2020](https://doi.org/10.5194/amt-13-3521-2020), 2020.
- 1021 [Ashpole, I., and Wiacek, A.: Land- and water-only Level 3 products from MOPITT TIR-NIR Version 8 CO](https://doi.org/10.5683/SP3/ERCG2H)
1022 [retrievals, https://doi.org/10.5683/SP3/ERCG2H, Borealis, V1, 2022](https://doi.org/10.5683/SP3/ERCG2H)
- 1023 Buchholz, R. R., Worden, H. M., Park, M., Francis, G., Deeter, M. N., Edwards, D. P., Emmons, L. K.,
1024 Gaubert, B., Gille, J., Martínez-Alonso, S., Tang, M., Kumar, R., Drummond, J. R., Clerbaux, C., George,
1025 M., Coheur, P-F., Hurtmans, D., Bowman, K. W., Luo, M., Payne, V. H., Worden, J. R., Chin, M., Levy,
1026 R. C., Warner, J., Wei, Z., Kulawik, S. S.: Air pollution trends measured from Terra: CO and AOD over
1027 industrial, fire-prone, and background regions, *Remote Sensing of Environment*, 256, 112275,
1028 <https://doi.org/10.1016/j.rse.2020.112275>, 2021.
- 1029 Buchholz, R. R., Park, M., Worden, H. M., Tang, W., Edwards, D. P., Gaubert, B., Deeter, M. N., Sullivan,
1030 T., Ru, M., Chin, M., Levy, R. C., Zheng, B., Magzamen, S.: New seasonal pattern of pollution emerges
1031 from changing North American wildfires, *Nature Communications* 13(2043),
1032 <https://doi.org/10.1038/s41467-022-29623-8>, 2022
- 1033 Deeter, M. N., Emmons, L. K., Francis, G. L., Edwards, D. P., Gille, J. C., Warner, J. X., Khattatov, B.,
1034 Ziskin, D., Lamarque, J.-F., Ho, S.-P., Yudin, V., Attié, J.-L., Packman, D., Chen, J., Mao, D. Drummond,
1035 J. R.: Operational carbon monoxide retrieval algorithm and selected results for the MOPITT instrument,
1036 *Journal of Geophysical Research*, 108(D14), 4399, <https://doi.org/10.1029/2002JD003186>, 2003.
- 1037 Deeter, M. N., Edwards, D. P., Gille, J. C., and Drummond, J. R.: Sensitivity of MOPITT observations to
1038 carbon monoxide in the lower troposphere, *Journal of Geophysical Research Atmospheres*, 112(24), 1–9,
1039 <https://doi.org/10.1029/2007JD008929>, 2007.
- 1040 Deeter, M. N., Martínez-Alonso, S., Edwards, D. P., Emmons, L. K., Gille, J. C., Worden, H. M., Pittman, J.
1041 V., Daube, B. C. and Wofsy, S. C.: Validation of MOPITT Version 5 thermal-infrared, near-infrared, and

- 1042 multispectral carbon monoxide profile retrievals for 2000-2011, *Journal of Geophysical Research*
1043 *Atmospheres*, 118(12), 6710–6725, <https://doi.org/10.1002/jgrd.50272>, 2013.
- 1044 Deeter, M. N., Martínez-Alonso, S., Edwards, D. P., Emmons, L. K., Gille, J. C., Worden, H.M., Sweeney,
1045 C., Pittman, J. V., Daube, B. C., and Wofsy, S. C.: The MOPITT Version 6 product: Algorithm
1046 enhancements and validation, *Atmospheric Measurement Techniques*, 7(11), 3623–3632,
1047 <https://doi.org/10.5194/amt-7-3623-2014>, 2014.
- 1048 Deeter, M. N., Edwards, D. P., Gille, J. C., and Worden, H. M.: Information content of MOPITT CO profile
1049 retrievals: Temporal and geographical variability, *Journal of Geophysical Research: Atmospheres*,
1050 120(24), 12723–12738, <https://doi.org/10.1002/2015JD024024>, 2015.
- 1051 Deeter, M. N., Edwards, D. P., Francis, G. L., Gille, J. C., Mao, D., Martínez-Alonso, S., Worden, H.M.,
1052 Ziskin, D., and Andreae, M. O.: Radiance-based retrieval bias mitigation for the MOPITT instrument:
1053 The version 8 product, *Atmospheric Measurement Techniques*, 12(8), 4561–4580,
1054 <https://doi.org/10.5194/amt-12-4561-2019>, 2019.
- 1055 Deeter, M., Francis, G., Gille, J., Mao, D., Martínez-Alonso, S., Worden, H., Ziskin, D., Drummond, J.,
1056 Commane, R., Diskin, G., and McKain, K.: The MOPITT Version 9 CO Product: Sampling Enhancements
1057 and Validation, *Atmos. Meas. Tech.*—~~Discuss.~~—[preprint], <https://doi.org/10.5194/amt-2021-370>,
1058 <https://doi.org/10.5194/amt-15-2325-2022>, in review, 2022†.
- 1059 Drummond, J. R., Zou, J., Nichitiu, F., Kar, J., Deschambaut, R., and Hackett, J.: A review of 9-year
1060 performance and operation of the MOPITT instrument, *Advances in Space Research*, 45(6), 760–774,
1061 <https://doi.org/10.1016/j.asr.2009.11.019>, 2010.
- 1062 Drummond, J. R., Hackett, J., and Caldwell, D.: Measurements of pollution in the troposphere (MOPITT),
1063 in: *Optical Payloads for Space Missions*, edited by: Shen-En Qian, Wiley and Sons, West Sussex, UK,
1064 639–652, 2016.
- 1065 Duncan, B. N., Logan, J. A., Bey, I., Megretskaia, I. A., Yantosca, R. M., Novelli, P. C., Jones, N.B., and
1066 Rinsland, C. P.: Global budget of CO, 1988 - 1997: Source estimates and validation with a global model,
1067 *Journal of Geophysical Research Atmospheres*, 112(22), D22301, <https://doi.org/10.1029/2007JD008459>,
1068 2007.
- 1069 Edwards, D. P., Halvorson, C. M., and Gille, J. C.: Radiative transfer modeling for the EOS Terra satellite
1070 Measurement of Pollution in the Troposphere (MOPITT) instrument, *Journal of Geophysical Research*
1071 *Atmospheres*, <https://doi.org/10.1029/1999JD900167>, 1999.
- 1072 Francis, G. L., Deeter, M. N., Martínez-Alonso, S., Gille, J. C., Edwards, D. P., Mao, D., Worden, H. M.,
1073 and Ziskin, D.: Measurement of Pollution in the Troposphere Algorithm Theoretical Basis Document:
1074 Retrieval of Carbon Monoxide Profiles and Column Amounts from MOPITT Observed Radiances (Level

1 to Level 2), Atmospheric Chemistry Observations and Modelling Laboratory, National Center for Atmospheric Research, Boulder, Colorado, downloaded from: https://www2.acom.ucar.edu/sites/default/files/mopitt/ATBD_5_June_2017.pdf, 2017.

Hedelius, J. K., Toon, G. C., Buchholz, R. R., Iraci, L. T., Podolske, J. R., Roehl, C. M., Wennberg, P. O., Worden, H. M., Wunch, D.: Regional and Urban Column CO Trends and Anomalies as Observed by MOPITT Over 16 Years, *Journal of Geophysical Research: Atmospheres*, 126(5), 1–18, <https://doi.org/10.1029/2020JD033967>, 2021.

Lamarque, J. F., Emmons, L. K., Hess, P. G., Kinnison, D. E., Tilmes, S., Vitt, F., Heald, C. L., Holland, E. A., Lauritzen, P. H., Neu, J., Orlando, J. J., Rasch, P. J., and Tyndall, G. K.: CAM-chem: Description and evaluation of interactive atmospheric chemistry in the Community Earth System Model, *Geoscientific Model Development*, 5(2), 369–411, <https://doi.org/10.5194/gmd-5-369-2012>, 2012.

MOPITT Algorithm Development Team: MOPITT (Measurements of Pollution in the Troposphere) Version 8 Product User’s Guide, Atmospheric Chemistry Observations and Modeling Laboratory, National Center for Atmospheric Research, Boulder, downloaded from: https://www2.acom.ucar.edu/sites/default/files/mopitt/v8_users_guide_201812.pdf, 2018.

[NASA/LARC/SD/ASDC, 2000a. MOPITT Derived CO \(Near and Thermal Infrared Radiances\) V008. Available at: https://doi.org/10.5067/TERRA/MOPITT/MOP02J_L2.008.](https://doi.org/10.5067/TERRA/MOPITT/MOP02J_L2.008)

[NASA/LARC/SD/ASDC, 2000. MOPITT CO gridded daily means \(Near and Thermal Infrared Radiances\) V008. Available at: https://doi.org/10.5067/TERRA/MOPITT/MOP03J_L3.008.](https://doi.org/10.5067/TERRA/MOPITT/MOP03J_L3.008)

Pan, L., Edwards, D. P., Gille, J. C., Smith, M. W., and Drummond, J. R.: Satellite remote sensing of tropospheric CO and CH₄: forward model studies of the MOPITT instrument, *Applied Optics*, 34(30), 6976. <https://doi.org/10.1364/ao.34.006976>, 1995.

Pan, L., Gille, J. C., Edwards, D. P., Bailey, P. L., and Rodgers, C. D.: Retrieval of tropospheric carbon monoxide for the MOPITT experiment, *Journal of Geophysical Research*, 103(D24), 32277. <https://doi.org/10.1029/98JD01828>, 1998.

Rodgers, C. D.: *Inverse Methods for Atmospheric Sounding, Theory and Practice*, World Scientific, Singapore, 2000.

Worden, H. M., Deeter, M. N., Edwards, D. P., Gille, J. C., Drummond, J. R., and Nédélec, P.: Observations of near-surface carbon monoxide from space using MOPITT multispectral retrievals, *Journal of Geophysical Research Atmospheres*, 115(18), 1–12, <https://doi.org/10.1029/2010JD014242>, 2010.

Worden, H. M., Deeter, M. N., Edwards, D. P., Gille, J., Drummond, J., Emmons, L. K., Francis, G., and Martínez-Alonso, S.: 13 years of MOPITT operations: Lessons from MOPITT retrieval algorithm development, *Annals of Geophysics*, 56(FAST TRACK 1), 1–5, <https://doi.org/10.4401/ag-6330>, 2014.